

## Nuclear processes in other universes: Varying the strength of the weak force

Alex R. Howe

*Department of Astronomy, University of Michigan, Ann Arbor, Michigan 48109, USA*

Evan Grohs

*Department of Physics, University of California Berkeley, Berkeley, California 94720, USA  
and Theoretical Division, Los Alamos National Laboratory, Los Alamos, New Mexico 87545, USA*

Fred C. Adams

*Department of Astronomy, University of Michigan, Ann Arbor, Michigan 48109, USA  
and Department of Physics, University of Michigan, Ann Arbor, Michigan 48109, USA*



(Received 9 July 2018; published 20 September 2018)

Motivated by the possibility that the laws of physics could be different in other regions of space-time, we consider nuclear processes in universes where the weak interaction is either stronger or weaker than observed. We focus on the physics of both big bang nucleosynthesis (BBN) and stellar evolution. For sufficiently ineffective weak interactions, neutrons do not decay during BBN, and the baryon-to-photon ratio  $\eta$  must be smaller in order for protons to survive without becoming incorporated into larger nuclei. For stronger weak interactions, neutrons decay before the onset of BBN, and the early Universe is left with nearly a pure hydrogen composition. We then consider stellar structure and evolution for the different nuclear compositions resulting from BBN, a wide range of weak force strengths, and the full range of stellar masses for a given universe. We delineate the range of this parameter space that supports working stars, along with a determination of the dominant nuclear reactions over the different regimes. Deuterium burning dominates the energy generation in stars when the weak force is sufficiently weak, whereas proton-proton burning into helium-3 dominates for the regime where the weak force is much stronger than in our Universe. Although stars in these universes are somewhat different, they have comparable surface temperatures, luminosities, radii, and lifetimes so that a wide range of such universes remain potentially habitable.

DOI: [10.1103/PhysRevD.98.063014](https://doi.org/10.1103/PhysRevD.98.063014)

### I. INTRODUCTION

The laws of physics include a number of fundamental constants with particular values that must be specified but cannot be derived from currently known theoretical considerations. At the same time, many cosmological models allow for the existence of other universes—regions of space-time that trace through independent evolutionary trajectories and are disconnected from our own [1–5]. Moreover, the values of the fundamental constants could, in principle, be different in these other universes. This scenario thus posits a vast ensemble of universes, often called the multiverse, where the various subregions sample the different possible versions of the laws of physics [1,6,7]. Many authors have suggested that sufficiently large variations in the laws of physics would result in a lifeless universe, so that only small changes to the fundamental constants are allowed [8–10]. The goal of this paper is to consider the effects of changing the strength of the weak nuclear force and assess the potential habitability of such scenarios.

Previous work has shown that universes where the weak force is absent entirely could still be habitable for a range of values of the other cosmological parameters and fundamental constants [11,12]. These papers considered particle physics models and cosmological issues [12], as well as numerical simulations of big bang nucleosynthesis (BBN) and stellar evolution [11]. However, previous treatments have not addressed the full implications for universes in which the weak force is weaker than in the Standard Model of particle physics, but still present, or cases where the weak force is stronger. This present paper addresses these more general cases by allowing the strength of the weak nuclear force to vary across the full range of possible values. We focus on nuclear processes, specifically, BBN and stellar evolution, and find the strengths of the weak force that allow for universes to be potentially habitable.

The strength of the weak interaction is a fundamental feature of the Standard Model of particle physics (for a textbook treatment, see [13]). The weak interaction

determines the rate of beta decay of free neutrons as well as those bound in nuclei. It also controls the rate of helium production in the  $pp$  chain for low-mass stars because the weak force must act to convert two of the protons into neutrons. Finally, the weak force determines the cross sections for neutrino interactions, which provide an energy drain from stellar interiors and play an important role in the successful detonation of supernova explosions. If the weak force is even weaker than in our Universe, neutron decay will be slower and neutrino interactions will be less effective. In the opposite case with stronger weak interactions, neutrons decay rapidly and neutrinos interact with larger cross sections. These processes affect the yields of light elements emerging from BBN and nuclear reactions in stellar interiors. Both of these processes are important for determining the potential habitability of a universe.

For the case of the weakless universe, BBN and stellar evolution play out as follows: The epoch of BBN determines the chemical composition of the Universe for the first generation of stars and has implications for further generations. If nuclear reactions are too effective during BBN, then a universe could process essentially all of its protons and neutrons into heavier elements, leaving no hydrogen behind to make water. In conventional BBN, neutrons start to decay before the onset of BBN so that protons outnumber the neutrons by a factor of 6–7 (depending on when the accounting is done). After essentially all of the neutrons are incorporated into nuclei, mostly helium, this mismatch leads to leftover protons [14]. In the absence of the weak force, however, neutrons do not decay. With equal numbers of protons and neutrons, the Universe faces the danger of burning all of its baryons into helium and heavier nuclei. This fate can be avoided if the nuclear reactions cannot proceed to completion during the brief window of time when nucleosynthesis takes place. In particular, lower baryon abundances lead to lower reaction rates so that even a weakless universe can retain protons. Previous work shows that if the baryon-to-photon ratio  $\eta$  is smaller by a factor of  $\sim 100$ , the helium and hydrogen abundances are the same as in our Universe [11,12]. Other chemical abundances are not the same, as more deuterium and helium-3 are produced and free neutrons remain. Later in cosmic history, these nuclear species play an important role in stellar evolution, which is primarily powered by deuterium burning in weakless universes.

With scenarios for both the conventional universe and the weakless universe worked out, this paper considers both the intermediate realm where the weak force is weaker than in our Universe and the opposite case where it is more effective. The weak force has both a strength set by the Fermi constant  $G_F \simeq 1.16 \times 10^{-5} \text{ GeV}^{-2} \simeq (293 \text{ GeV})^{-2}$ , and a range determined by the mass scale of intermediate vector bosons  $M_W \sim 80 \text{ GeV}$ . In this treatment, we keep the masses of all particles the same as in our Universe, but we allow the coupling strength and equivalently the

Fermi constant to vary, as outlined in Sec. II. One important quantity in the problem is the neutron lifetime  $\tau_n$ , which is mediated by the weak force, and can be written in the form

$$\tau_n^{-1} = \frac{G_F^2}{2\pi^3} (1 + g_A^2) m_e^5 \lambda_0, \quad (1)$$

where  $g_A \approx 1.26$  is the axial-vector coupling for nucleons and where  $\lambda_0 \approx 1.636$  is a dimensionless parameter. Here we specify variations in the weak interaction strength in terms of the neutron lifetime. The limit  $\tau_n \rightarrow \infty$  corresponds to the weakless universe.

This paper is organized as follows. We first discuss the physical implications of changing the Fermi constant, equivalently, the neutron lifetime, in Sec. II. Using a state-of-the-art numerical code [15], Sec. III considers the effects of changing  $\tau_n$  on the output from BBN. In this context, we allow the baryon-to-photon ratio  $\eta$  to vary also. Again using a state-of-the-art numerical treatment [16], we consider the effects of changing  $\tau_n$  on stellar evolution. In this context, stars of different masses are affected differently, and even the allowed range of stellar masses can vary. Section IV thus considers stellar evolution over the full  $(\tau_n, M_*)$  parameter space and finds the regions that allow for working stars, as well as the dominant nuclear-reaction chains in each regime. In Sec. V, we examine the later stages of stellar evolution and the chemical evolution and potential habitability of the resulting universes. The paper concludes in Sec. VI with a summary of our results and a discussion of their implications.

## II. CONSIDERATIONS FROM FUNDAMENTAL PHYSICS

It is not clear what effect a stronger weak interaction would have on nuclear structure. Clearly, if the weak force approaches the strength of the strong force, it ceases to be perturbative, and our models of nuclear structure are no longer viable. In addition, the nonlinear behavior is complicated by the fact that the relative strength of the strong and weak forces varies with the energy scale in question. We can write the weak coupling constant in the low-energy limit in the form

$$\alpha_w = G_F m_p^2 \sim 10^{-5}, \quad (2)$$

where the neutron lifetime  $\tau_n \propto G_F^{-2}$  as given by Eq. (1).

Under the conditions in stellar interiors where nuclear reactions take place, the weak force is less effective than the strong force by  $\sim 13$  orders of magnitude. As a result, the neutron lifetime could, in principle, be as short as  $\tau_n \sim 10^{-22} \text{ s}$  before nuclear reactions are changed significantly. As an example, consider the last step in the  $pp$  chain where two  ${}^3\text{He}$  nuclei come together. The resulting compound nucleus is beryllium-6, which in our Universe disintegrates into  ${}^4\text{He}$  and two free protons via the strong interaction.

If the neutron lifetime is on the order of the strong-interaction timescale, beryllium-6 would decay into lithium-6 at a rate competitive with the strong branch. Such a scenario would have profound implications for main-sequence stars.

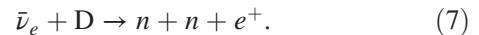
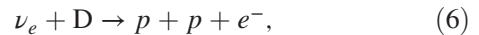
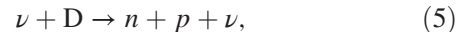
Note that at less extreme values of  $\tau_n$  (equivalently,  $G_F$ ), beta decay ( $(\beta)$  decay) will occur more readily inside nuclei than in our Universe. For all radioactive nuclei subject to  $(\beta)$  decay, the half-lives will be much shorter. For sufficiently small values of  $\tau_n$ , only the stable isotope for a given mass number  $A$  will have an appreciable abundance. In standard BBN, for example, the  $A = 3$  isobar has contributions from both tritium T and  ${}^3\text{He}$ . Much of the  $A = 3$  material is eventually synthesized to  ${}^4\text{He}$  through strong and electromagnetic reactions. T only has a single proton and so will correspondingly have a smaller Coulomb barrier than the  $Z = 2$  nucleus of  ${}^3\text{He}$ . If the weak interaction immediately transmutes T into  ${}^3\text{He}$ , the rates for  ${}^4\text{He}$  synthesis will decrease, which may result in a smaller abundance of  ${}^4\text{He}$  than the abundance inferred from the neutron-to-proton ratio. Those “missing” neutrons would be in  ${}^3\text{He}$  nuclei which could affect stellar nucleosynthesis at later epochs. However, a weak interaction strong enough to transmute T into  ${}^3\text{He}$  on BBN timescales would also hold the neutron-to-proton ratio at equilibrium until late times. As a result, there may be few neutrons that survive the BBN epoch, and so the relative abundances of  ${}^3\text{He}$  and  ${}^4\text{He}$  could be unimportant to the first generation of nearly-pure-hydrogen stars.

These factors related to weak versus strong nuclear reactions may be moot, however, if the strength of the weak force approaches that of the electromagnetic force. If the two forces remain unified in an electroweak force, then the photon and  $Z^0$  bosons convert to the  $W_3$  and  $B_0$  eigenstates, and again, nucleosynthesis will not operate normally, particularly the  $D(p, \gamma){}^3\text{He}$  reaction in the  $pp$  chain. At the scale of nuclear reactions in stars, this unification occurs at  $\tau_n \sim 10^{-15}$  s. It is not clear what form nuclear physics will take in such weakful universes.

The next problem with a weakful universe is that neutrino interaction cross sections will be nontrivial at stellar and BBN conditions. Neutrinos will behave more like photons in these environments and will significantly affect nuclear processes. In our Universe, the cumulative optical depth of neutrinos through the period of BBN is  $\sim 10^{-12}$ . The neutrino interaction cross section scales inversely with the neutron lifetime, so if we set  $\tau_n \lesssim 10^{-9}$  s, then neutrino interactions will exert a significant effect on BBN. Weak nuclear reactions will maintain nuclear statistical equilibrium (NSE) well into the BBN epoch, and additional charged-current reactions will be involved, e.g.,



Conversely, high-energy neutrino spallation can dissociate deuterons through neutral or charged-current interactions



With these reactions occurring, we cannot take our zeroth-order estimate of a BBN yield of 100% hydrogen for very weakful universes.

For stars, the neutrino opacity limit is even more stringent. The optical depth of the Sun to neutrinos is  $10^{-9}$  [17]. A  $1 M_\odot$  star in a weakful universe would become optically thick to neutrinos at  $\tau_n \sim 10^{-6}$  s. Strong and electromagnetic interactions will still function normally under such circumstances, but the neutrino bath in the stellar core will change the progression of stellar evolution, and we can no longer accurately simulate such objects using stellar evolution codes such as MESA, as neutrino interactions would need to be included in its equation of state and nuclear-reaction network. (It is possible to include the effects of neutrino scattering in MESA, but this is beyond the scope of the present paper.) Nonetheless, it is entirely possible that long-lived stars and life-supporting planets could exist in such a universe.

In addition to neutrino interactions, changes in the weak interaction cross section will lead to corresponding changes in the abundance of dark matter and its self-interactions within dark matter halos. Under the usual assumptions for the thermal production of weakly interacting dark matter particles (WIMPs), the predicted abundance scales as [14]  $\Omega_X \propto \langle \sigma v \rangle^{-1} \propto G_F^{-2} m_X^{-2}$ , where  $m_X$  is the mass of the dark matter particle, and  $G_F$  is the Fermi constant. The usual WIMP miracle is that we expect new particles (dark matter) to have masses roughly comparable to the weak scale (100 GeV to 1 TeV), which gives us  $\Omega_X$  of order unity. Here we are changing the value of  $G_F$ , which would change the expected inventory of dark matter. Since the nature of dark matter remains unknown, further discussion is beyond the scope of this paper.

Our analysis so far has focused on weakful universes with shorter neutron lifetimes. For longer neutron lifetimes, we maintain the assumption that only the strong and electromagnetic forces determine binding energies and stability. A longer neutron lifetime will decrease weak interaction rates at all energy scales, and we expect convergence to the class of weakless universes in the limit  $\tau_n \rightarrow \infty$ . In this paper, we will take two ranges of  $\tau_n$  for BBN and stars. For BBN, we take  $\tau_n$  to be in the range between 1 and  $10^8$  s. If  $\tau_n > 10^8$  s, then the weak interaction would fall out of equilibrium during the

quark-hadron transition in the early Universe, which we do not consider quantitatively. For  $\tau_n < 1$  s, we expect the primordial mass fraction of hydrogen to be nearly equal to unity as long as nuclear structure remains similar to that for our Universe. We expand the range of  $\tau_n$  for our stellar calculations to be between  $10^{-6}$  and  $10^7$  s, where the lower limit ensures we can still approximate neutrinos as free-streaming for a  $1 M_\odot$  star. If  $\tau_n > 10^7$  s, the main sequences are virtually identical until a point where the CNO cycle ceases to be able to power stars.

### III. BIG BANG NUCLEOSYNTHESIS WITH DIFFERENT STRENGTH OF THE WEAK INTERACTION

#### A. Model

The weak interaction plays a role in multiple aspects of BBN. Our motivation is to investigate how changes to  $G_F$  will impact BBN, but there exist other alternative methods for this pursuit. Reference [18] considers what limits primordial and stellar nucleosynthesis can place on the Higgs mass scale, whereas Refs. [19,20] consider the weak scale in BBN by changing the Higgs vacuum expectation value (VEV). Changing the Higgs VEV will change  $G_F$  and the fermion masses of the Standard Model, assuming that the Yukawa couplings are preserved while changing the Higgs VEV. Both Refs. [19,20] consider how the nuclear binding energies would change with different quark masses by using results from lattice QCD (see references in Ref. [19]). In this work, we will only change  $G_F$  in our calculations. In other words, we preserve the fermion masses and binding energies by changing the Yukawa couplings to correspond to changes in  $G_F$ .

We base our BBN calculations on Refs. [15,21,22]. The standard code from Ref. [21] assumes that the neutrinos are decoupled from the electromagnetic plasma at all times encompassed by the code (see, in particular, Ref. [23]). If we change the strength of the weak interaction by changing  $G_F$ , the neutrinos will decouple at either earlier ( $G_F < G_{F,0}$ ) or later ( $G_F > G_{F,0}$ ) times where  $G_{F,0}$  is the value of the Fermi constant in our Universe. We can approximate neutrino decoupling by comparing the rate of scattering to that of the Hubble expansion rate. Equations (3) and (5) in Ref. [24] give expressions for the annihilation of neutrinos into charged leptons  $\Gamma$  and also that of the Hubble expansion rate  $H$ ,

$$\Gamma = \frac{16G_F^2}{\pi^3} (g_L^2 + g_R^2) T^5, \quad (8)$$

$$H = 1.66g_\star^{1/2} \frac{T^2}{m_{\text{pl}}}, \quad (9)$$

where  $(g_L^2 + g_R^2)$  is the coupling of neutrinos to charged leptons (dependent on neutrino flavor),  $g_\star$  is the effective

spin statistic [14],  $m_{\text{pl}}$  is the Planck mass, and  $T$  is the plasma temperature. If we take  $g_\star = 43/4$  and equate Eqs. (8) and (9), we can solve for the temperature  $T_D$ , at which neutrinos decouple from the electromagnetic plasma. Reference [24] finds  $T_D(\nu_e) \simeq 2.4$  MeV for electron-flavor neutrinos and  $T_D(\nu_\mu, \nu_\tau) \simeq 3.7$  MeV for  $\mu$  and  $\tau$  flavor. For our purposes, it is adequate to use the same value for all three flavors, which we pick to be  $T_{D,0} = 3.0$  MeV, where the 0 subscript denotes the value in our Universe. We can determine the scaling of  $T_D$  with  $G_F$  or the neutron lifetime  $\tau_n$  from Eqs. (8) and (9),

$$T_D = T_{D,0} \left( \frac{G_{F,0}}{G_F} \right)^{2/3} \quad (10)$$

$$= T_{D,0} \left( \frac{\tau_n}{\tau_{n,0}} \right)^{1/3}. \quad (11)$$

Two problems arise with our scaling law in Eq. (11). First,  $T_{D,0}$  is a function of  $g_\star$  from Eq. (9). If we increase  $\tau_n$  to large values, neutrinos will decouple when there are non-negligible amounts of  $\mu$  and  $\bar{\mu}$  particles in the electromagnetic plasma. This complication would increase  $g_\star$  which we did not take into account in Eq. (11). Second, and related to the first point, if there are  $\mu$  particles around, that would provide more scattering targets for neutrinos. The result would be an increase in the  $(g_L^2 + g_R^2)$  factor in a flavor-dependent manner for all three flavors. The temperature  $T_{D,0} \sim [g_\star / (g_L^2 + g_R^2)]^{1/3}$ , so the changes in the two quantities act to offset one another, although the ratio would not be exactly preserved. A proper calculation of the ratio is nontrivial as  $\mu$  and  $\bar{\mu}$  do not fully contribute to either  $g_\star$  or the coupling constants in the temperature range where  $T_{D,0}$  may reside. For simplicity, we will use the scaling in Eq. (11) to set the decoupling temperature in our BBN calculations.

Another complication arises if we take a long neutron lifetime. Neutrons and protons are formed during the quark-hadron transition of  $\sim 170$  MeV [25]. Using the scaling in Eq. (11), the decoupling temperature and the quark-hadron transition coincide for  $\tau_n \sim 10^8$  s. At this point, neutrinos would decouple before neutrons and protons exist and would not directly influence the neutron-to-proton ratio (denoted  $n/p$ ). The resulting primordial nucleosynthesis is much like that of the weakless universe [11] with neutrinos acting like dark radiation [26]. Therefore, we limit our BBN calculations to  $\tau_n < 10^8$  s.

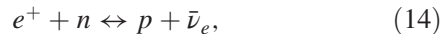
The presence of  $\mu$  particles and the modified neutrino decoupling epoch present two challenges. First,  $\mu$  particles must be added to the electromagnetic plasma which will change the equation of state. Equation (D28) in Ref. [23] gives the time derivative of the plasma temperature during BBN,

$$\frac{dT}{dt} = -3H \left( \frac{d\rho_{\text{pl}}}{dT} \right)^{-1} \left( \rho_{\text{pl}} + P_{\text{pl}} + \frac{1}{3H} \frac{dQ}{dt} \Big|_T \right), \quad (12)$$

where  $\rho_{\text{pl}}$  is the energy density of the plasma (less baryons),  $P_{\text{pl}}$  is the pressure exerted by all plasma components,  $dQ/dt|_T$  is the heat lost from the plasma due to nucleosynthesis, and  $d\rho_{\text{pl}}/dT$  is the temperature derivative of the plasma components (including baryons). In Ref. [23], the plasma components are assumed to be photons, electrons, positrons, and baryons. We must start our calculation when there are  $\mu$  and  $\bar{\mu}$  present, so we must add these terms to the energy density, pressure, and temperature derivative of energy density. We assume that the  $\mu$  particles are in thermal equilibrium with zero chemical potential. By the time we reach nuclear freeze-out ( $T \sim 100$  keV), the equilibrium abundance of  $\mu$  particles is  $Y_\mu \sim e^{-m_\mu/T}$ , which is negligible compared to the electron and positron abundances.

Second, neutrinos also need to be included in the electroweak plasma equation of state if they do not decouple until late times. For temperatures larger than  $T_D$ , neutrinos are included in all three plasma terms in Eq. (12). For temperatures lower than  $T_D$ , they are decoupled and their effective temperature redshifts with increasing scale factor. We call this temperaturelike quantity the comoving temperature parameter and denote it  $T_{\text{cm}}$  [see Eq. (1) in Ref. [27]].

The standard nuclear-reaction network of Ref. [23] contains two sets of weak rates: the neutron-to-proton rates (denoted  $n \leftrightarrow p$  rates) and the nuclear  $\beta$ -decay rates. The six processes which interconvert neutrons to protons are given schematically as



where the forward arrow indicates proton creation, and the reverse arrow indicates neutron creation. Each one of the six  $n \leftrightarrow p$  rates [corresponding to a process in Eqs. (13)–(15)] scale the same way with  $G_F$  [28]

$$\lambda \propto \frac{G_F^2 (1 + 3g_A^2)}{2\pi^3} I, \quad (16)$$

where  $g_A$  is the axial-vector coupling, and  $I$  is a phase-space integral with units of  $[\text{MeV}^5]$  and depends on the specific process in Eqs. (13)–(15). Equation (16) for free-neutron decay [the forward process in Eq. (15)] is consistent with Eq. (1) if we take  $I = m_e^5 \lambda_0$  at zero temperature. To wit, we equate the free-neutron decay rate at zero temperature with the vacuum decay rate, namely,  $1/\tau_n$ , to give a quantitative relationship between  $G_F$  and the neutron

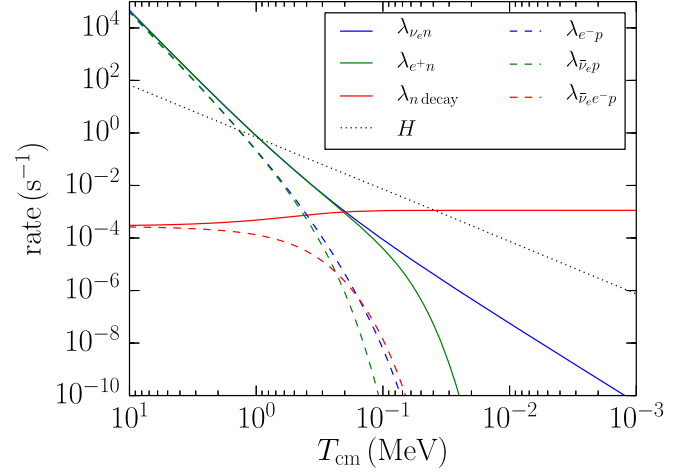
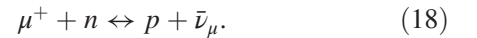


FIG. 1. The  $n \leftrightarrow p$  rates in standard BBN versus decreasing comoving temperature parameter (equivalent to increasing time) from Ref. [28]. Plotted for comparison is the Hubble expansion rate  $H$  as a dotted black line.

lifetime [see Eq. (26) in Ref. [28]]. Once we have a value of  $G_F$  from an input value of  $\tau_n$ , we can calculate all six  $n \leftrightarrow p$  rates at all temperatures. Figure 1 is a plot from Ref. [28] and gives the six  $n \leftrightarrow p$  rates of standard BBN as a function of decreasing comoving temperature parameter  $T_{\text{cm}}$ .

If neutrinos decouple from the electromagnetic plasma at high temperatures, it is possible for there to be other charged-current interactions involving  $\mu$  particles, namely,



Processes (17) and (18) are the  $\mu$ -flavor analogs of (13) and (14), respectively. We do not include a three-body process with  $\mu$  leptons in analogy with the reverse reaction in process (15), and there is no free-neutron-decay process into a state with muons. To calculate the forward and reverse rates for Eqs. (17) and (18), we use the same form of the scattering amplitude as we did for Eqs. (13)–(15) [29]. Furthermore, we use the same Coulomb and zero-temperature corrections for both the  $\mu$  flavor and  $e$  flavor [30,31]. The key difference between the  $\mu$ -flavor and  $e$ -flavor rates are the mass thresholds. The neutron-proton mass difference  $\delta m_{np}$  is approximately 1.3 MeV, whereas the electron mass is  $m_e \sim 0.5$  MeV. As  $\delta m_{np} > m_e$ , there are no energy thresholds for the three forward rates in Eqs. (13)–(15), while there are thresholds for the three reverse rates. The muon mass is  $m_\mu \sim 106$  MeV and so is larger than  $\delta m_{np}$ . Therefore, the forward process of Eq. (17) does have a threshold, while the reverse process does not. For Eq. (18), there is a threshold for the reverse

process and no threshold for the forward process, similar to the  $e$ -flavor analog of Eq. (14).

The nuclear  $\beta$ -decay rates of the light nuclei are similar to the  $n \leftrightarrow p$  rates. Beta decay is a charged-current process with an amplitude which depends on  $G_F^2$ . A difficulty in calculating expressions for ( $\beta$ ) decay is that there exists an amplitude for nuclear transitions which do not have analytic forms. We will assume that whatever form the nuclear matrix element takes, it is independent of  $G_F$  for the range of values we explore here. Therefore, we scale the  $\beta$ -decay rates the same way we scale the  $n \leftrightarrow p$  rates, namely,  $G_F^2 \propto 1/\tau_n$ . In practice, our nuclear-reaction network employs only one light-nuclei  $\beta$ -decay rate, that of tritium decaying to  ${}^3\text{He}$ . In our Universe,  $\tau_T \simeq 10$  yr, which is much longer than BBN timescales. For the tritium decay rate to be important during primordial nucleosynthesis,  $\tau_n$  would need to be smaller by roughly 6 orders of magnitude.

The final BBN ingredient where neutrinos play a role is in the total energy density. The Hubble expansion rate is proportional to the square root of the total energy density  $\rho$ . All of the light-nuclide yields are functions of the nuclear-reaction rates and the Hubble expansion rate. Helium-4 is especially sensitive with a faster expansion rate increasing the primordial mass fraction denoted  $Y_p$ . We adopt the notation of the cosmological observable  $N_{\text{eff}}$  to characterize the neutrino energy density [32]

$$\rho_{\text{rad}} = \left[ 2 + \frac{7}{4} \left( \frac{4}{11} \right)^{4/3} N_{\text{eff}} \right] \frac{\pi^2}{30} T^4, \quad (19)$$

where  $\rho_{\text{rad}}$  is the radiation energy density, and  $T$  is the plasma temperature. We can relate the neutrino energy density directly to  $N_{\text{eff}}$  by taking the radiation energy density as the sum of the neutrino and photon energy densities

$$\rho_{\text{rad}} = \rho_\gamma + \rho_\nu \Rightarrow \rho_\nu = \frac{7}{4} \left( \frac{4}{11} \right)^{4/3} N_{\text{eff}} \frac{\pi^2}{30} T^4, \quad (20)$$

$$\Rightarrow N_{\text{eff}} = \frac{4}{7} \left( \frac{11}{4} \right)^{4/3} \frac{\rho_\nu}{\frac{\pi^2}{30} T^4}. \quad (21)$$

In this paper, we always assume the neutrinos have Fermi-Dirac distributions with temperature parameters equal to the comoving temperature parameter  $T_{\text{cm}}$ . Therefore, we can write  $\rho_\nu$  as a function of  $T_{\text{cm}}$  and solve for  $N_{\text{eff}}$  in terms of the ratio  $T_{\text{cm}}/T$ ,

$$\rho_\nu = 6 \frac{7 \pi^2}{8 \cdot 30} T_{\text{cm}}^4 \Rightarrow N_{\text{eff}} = 3 \left[ \left( \frac{11}{4} \right)^{1/3} \frac{T_{\text{cm}}}{T} \right]^4. \quad (22)$$

To calculate the freeze-out ratio of  $T_{\text{cm}}/T$ , we use entropy arguments [14]

$$\frac{T_{\text{cm}}}{T} \Big|_{\text{f.o.}} = \left( \frac{g_{\star S, \text{f.o.}}}{g_{\star S, \text{dec}}} \right)^{1/3}, \quad (23)$$

where  $g_{\star S}$  is the entropic degrees of freedom at a particular epoch. The f.o. subscript denotes the electromagnetic freeze-out epoch when photons are the only plasma particles remaining. The dec subscript denotes the neutrino decoupling epoch. We will consider two limits of neutrino decoupling to obtain analytic values of the freeze-out ratio of the temperaturelike quantities: early decoupling with muons present and late decoupling with no electrons present. In both limits, only photons remain at freeze-out so  $g_{\star S, \text{f.o.}} = 2$ . If muons annihilate after neutrino decoupling

$$g_{\star S, \text{dec}} = 9 \Rightarrow \frac{T_{\text{cm}}}{T} \Big|_{\text{f.o.}} = \left( \frac{2}{9} \right)^{1/3} \Rightarrow N_{\text{eff}} \simeq 1.56, \quad (24)$$

and if electrons annihilate before decoupling

$$g_{\star S, \text{dec}} = 2 \Rightarrow \frac{T_{\text{cm}}}{T} \Big|_{\text{f.o.}} = 1 \Rightarrow N_{\text{eff}} \simeq 11.56. \quad (25)$$

If the neutrinos decouple during either  $\mu^\pm$  or  $e^\pm$  annihilation, then  $N_{\text{eff}}$  will be between the two values calculated above.  $N_{\text{eff}}$  is close to 3.0 if neutrinos decouple in the interlude between the two annihilation epochs.

## B. Results

Standard BBN requires the baryon content of the Universe as input. We adopt the nomenclature of Ref. [21] and use the baryon-to-photon ratio  $\eta$  given as a ratio of baryon and photon number densities

$$\eta \equiv \frac{n_b}{n_\gamma}. \quad (26)$$

We do not consider how varying the weak interaction would modify the baryon content of the Universe. Thermal leptogenesis of Ref. [33] has a dependence on the mass scale in the seesaw mechanism, and so it is unknown if a different weak scale would change this particular model of leptogenesis. The Akhmedov-Rubakov-Smirnov (ARS) model of leptogenesis [34] is dependent on the Higgs VEV, but it also has dependences on many other parameters, e.g., Yukawa couplings. The resulting baryon asymmetry from ARS leptogenesis may still be unchanged in a large section of its parameter space. (See Refs. [35,36] for reviews on different leptogenesis scenarios.) Our calculations assume that  $\eta$  and  $G_F$  are independent of one another, and we will vary both to explore the parameter space. For completeness, note also that changing the Higgs VEV can result in instability of the vacuum and could thus affect the potential viability of the Universe [37].

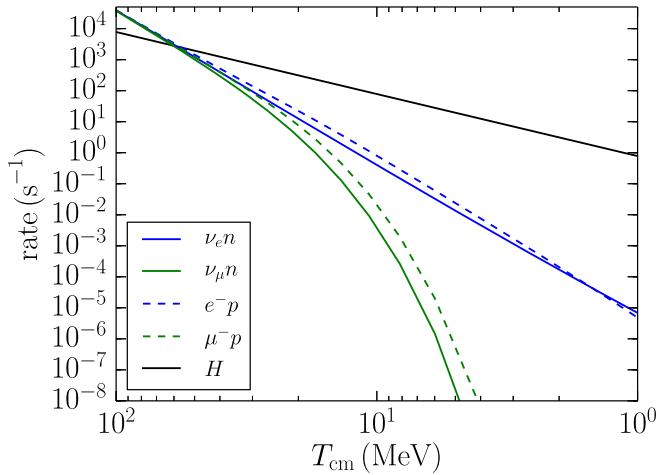


FIG. 2. Various  $n \leftrightarrow p$  rates and the Hubble expansion rate plotted against the comoving temperature parameter,  $T_{\text{cm}}$ . The neutron lifetime for this case is  $\tau_n = 10^8$  s, and the baryon-to-photon ratio is  $\eta = 6 \times 10^{-10}$ . Blue curves correspond to rates within the  $e$ -type leptons. Green curves correspond to rates within the  $\mu$ -type leptons. The solid blue (green) curves correspond to the forward rates of Eq. (13) [(17)], whereas the dashed blue (green) curve corresponds to the reverse rate of Eq. (13) [(17)]. Plotted for comparison is the Hubble expansion rate as a dotted black line.

We first compare the neutron-to-proton rates for  $e$  and  $\mu$  flavor at large  $\tau_n$ . Figure 2 shows various  $n \leftrightarrow p$  rates plotted against  $T_{\text{cm}}$ . We choose  $10^8$  s for the neutron lifetime, and a baryon-to-photon ratio the same as in our Universe, namely,  $\eta \simeq 6 \times 10^{-10}$  [38]. The baryon-to-photon ratio has little effect on the shape of the curves in Fig. 2 for  $\eta \ll 1$ . The blue curves correspond to rates which involve  $e$ -type leptons, namely,  $\nu_e n \leftrightarrow p e^-$ . The solid curve is the forward rate (neutron destruction), and the dashed curve is the reverse rate (neutron production). The green curves correspond to rates which involve  $\mu$ -type leptons, namely,  $\nu_\mu n \leftrightarrow p \mu^-$ , with the same nomenclature for solid versus dashed line style. Plotted for comparison is the Hubble expansion rate  $H$  as a solid black line. Although the  $n \leftrightarrow p$  rates fall below  $H$ ,  $n/p$  still evolves on long timescales, and so the muon contribution to  $n/p$  is non-negligible. Decreasing the neutron lifetime would increase all four  $n \leftrightarrow p$  rates (equivalent to shifting the blue and green curves upwards in Fig. 2) while preserving  $H$ . Freeze-out would occur later, and the contribution from Eqs. (17) and (18) to  $n/p$  would be less significant. Notice the general trend that all of the  $n \leftrightarrow p$  rates are roughly equal at high temperature. At high enough temperature, the three mass scales of interest (electron, muon, and neutron-proton difference) are either small or comparable to the temperature. Therefore, the charged leptons and neutrinos are relativistic, and the amount of available phase space is the same for all four rates. At lower temperatures, the muon

mass is important, and the rates involving muon-type leptons become negligible.

We did not plot the rates from Eq. (18) on Fig. 2. As the muon mass is much larger than the neutron-proton mass difference, the forward rate of Eq. (18), namely,  $\mu^+ n \rightarrow p \bar{\nu}_\mu$ , is nearly equal to  $\mu^- p \rightarrow n \nu_\mu$ . The two curves are coincident if they had both been plotted on Fig. 2. The reverse rate of (18) suffers from a large threshold in creating the muon mass, so it is always subsidiary to that of the forward rate.

The mass thresholds in the  $n \leftrightarrow p$  rates of Eqs. (13)–(15), (17), and (18) manifest differently for larger  $\tau_n$  than the value in our Universe. The mass hierarchy is  $m_\mu > \delta m_{np} > m_e$ . When a neutron becomes a proton, there is enough energy to make an electron. Conversely, a muon incident upon a proton has enough energy to create the neutron. As a result, there are thresholds in the reverse rate of Eq. (13) of the  $e$  type. For the  $\mu$  type, there is a threshold in the forward rate of Eq. (17). Figure 2 shows that the dashed green line (no threshold) has a larger rate than the solid green line (threshold of  $m_\mu - \delta m_{np}$ ). What is interesting is that the blue dashed line (threshold of  $\delta m_{np} - m_e$ ) is larger than the blue solid line (no threshold) over multiple Hubble times—opposite to the behavior of the  $\mu$ -type rates and different than our Universe (see Fig. 1). This is primarily due to the fact that the neutrinos thermally decoupled from the  $e^\pm$ ,  $\mu^\pm$  plasma at a temperature  $T_D \sim 100$  MeV. As the  $\mu^\pm$  annihilate, they produce  $e^\pm$  pairs and photons which heat the electromagnetic plasma but not the neutrino seas. The  $\nu_e$  are at a lower temperature, and so the forward rate of  $\nu_e n \leftrightarrow p e^-$  is smaller than the reverse rate. Figure 2 shows that the trend eventually reverses at low enough temperature once the threshold for the reverse rate becomes significant.

Figure 3 gives  $N_{\text{eff}}$  as a function of  $\tau_n$  for  $\eta = 6 \times 10^{-10}$ . The curve for  $N_{\text{eff}}$  versus  $\tau_n$  is independent of the specific value of  $\eta$  for  $\eta \ll 1$ . For large  $\tau_n$ , neutrinos decouple before the epoch of  $\mu^\pm$  annihilation, and so  $N_{\text{eff}}$  is smaller than 3.0.  $N_{\text{eff}}$  plateaus to a value of  $\simeq 1.5$  for large  $\tau_n$ , congruent with the value in Eq. (24). The plateau would not be an asymptote as even larger  $\tau_n$  would imply earlier decoupling periods when free quarks and  $\tau$  particles are still present. Our Universe sits on the plateau of  $N_{\text{eff}} \gtrsim 3.0$  in the domain  $10\text{s} < \tau_n < 10^5$  s. We have assumed that the charged leptons are always given by equilibrium distributions

$$n_\ell/n_\gamma \propto \left(\frac{m_\ell}{T}\right)^{3/2} e^{-m_\ell/T}, \quad (27)$$

where  $n_\ell$  is the number density and  $m_\ell$  the mass of the charged lepton, and we have assumed that we can describe the charged leptons with Maxwell-Boltzmann statistics—appropriate for late times when the charged leptons are annihilating. The decrease in  $N_{\text{eff}}$  at  $\tau_n \sim 10^5$  s corresponds

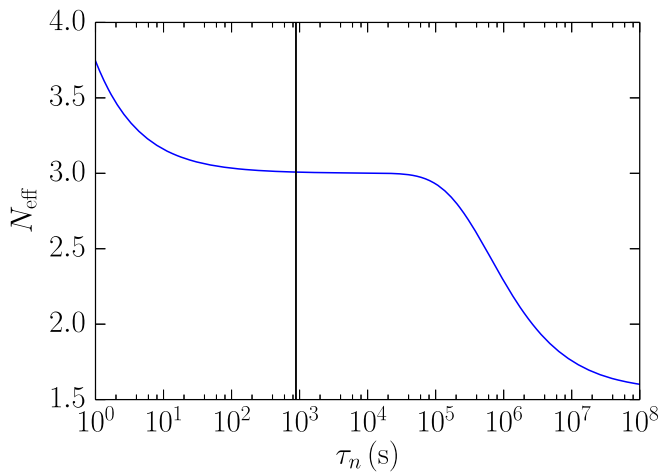


FIG. 3. Number of effective degrees of freedom  $N_{\text{eff}}$  [defined in Eq. (20)] as a function of the mean neutron lifetime  $\tau_n$ . The baryon-to-photon ratio is taken to be  $\eta = 6 \times 10^{-10}$  for all cases shown here. The black line indicates our Universe. Note that  $N_{\text{eff}}$  is nearly constant over a wide range of  $\tau_n$  so that our Universe is not fine-tuned in this regard.

to the end of  $\mu^\pm$  annihilation, whereas the increase in  $N_{\text{eff}}$  at  $\tau_n \sim 10$  s corresponds to the beginning of  $e^\pm$  annihilation. Therefore, the length of this range is a function of the difference in the electron and muon rest masses, although there is no simple scaling as we must compare the end of  $\mu^\pm$  annihilation with the beginning of  $e^\pm$  annihilation, and both epochs span multiple Hubble times. The location of our Universe on the plateau informs us that the energy scale of neutrino decoupling falls between the electron and muon rest masses, as indicated by the  $m_e/T$  scaling in the exponential of Eq. (27). The final point to make for Fig. 3 is that for small  $\tau_n$ ,  $N_{\text{eff}}$  steadily increases above 3.0. Had we gone to even smaller values of  $\tau_n$ , we would have seen another plateau at  $N_{\text{eff}} \approx 11.5$ , consistent with Eq. (25). Specifically,  $\tau_n \lesssim 3 \times 10^{-6}$  s would put neutrino decoupling after  $e^\pm$  annihilation. In the case of small  $\tau_n$ , the plateau at  $N_{\text{eff}} \approx 11.5$  would also be an asymptote, as there are no other particles left to annihilate before photon decoupling.

Figures 2 and 3 both depict neutrino physics in the early Universe. The neutrinos change  $n/p$ , which eventually affects the primordial abundances. Figure 4 shows  $\tau_n$  versus  $\eta$  at contours of constant single-proton hydrogen mass fraction,  $X_{1\text{H}}$ . The value of  $\eta$  is the final baryon-to-photon ratio after  $e^\pm$  annihilation, consistent with what an observer would measure in the cosmic microwave background. We place a red star at the value of  $\eta$  and  $\tau_n$  which correspond to our Universe. The red star falls on the 75% contour, in line with standard BBN calculations. For small  $\tau_n$ , the contours steadily approach an asymptote of unity as few neutrons survive the BBN epoch. There exist two general trends: increasing  $\eta$  gives fewer free protons, and increasing  $\tau_n$  also

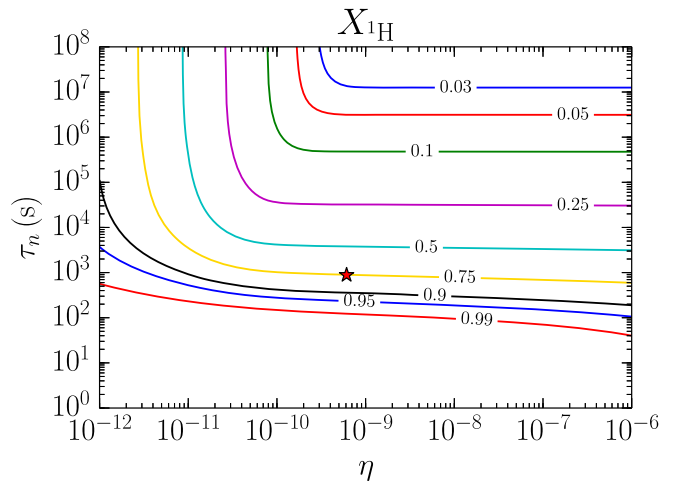


FIG. 4. Contours of constant mass fraction of single-proton hydrogen in the  $(\eta, \tau_n)$  plane, where  $\eta$  is the baryon-to-photon ratio and  $\tau_n$  is the mean neutron lifetime (in seconds). The red star indicates the location of our Universe in the diagram. The mass fraction of hydrogen approaches unity in the limit of small  $\tau_n$  in the bottom part of the figure, where BBN produces few nuclei. Universes can be rendered sterile in the upper right part of the diagram (large  $\eta$  and  $\tau_n$ ), where most of the protons are processed into other nuclei and few are left to supply the Universe with water.

gives fewer free protons. The latter trend is consistent with the scaling that a weaker weak force allows  $n/p$  to go out of equilibrium at earlier times and, hence, larger values. Fewer total protons implies fewer free protons survive nuclear freeze-out. A larger  $\eta$  implies faster nuclear reactions and delays nuclear freeze-out to later times. This trend is present for small to intermediate values of  $\eta$  in Fig. 4. For larger values of  $\eta$ , the nuclear reactions incorporate the free neutrons into heavier nuclides, and the free-proton mass fraction is stagnant with increasing  $\eta$ .

For large  $\eta$ , we can make a stronger statement than a constant  $X_{1\text{H}}$  and say  $n/p$  is constant with large  $\eta$ . Figure 5 shows contours of a constant  ${}^4\text{He}$  mass fraction in the  $\eta$  versus  $\tau_n$  parameter space. The contours in the top right of the parameter space (at large  $\eta$  and large  $\tau_n$ ) are equal to  $1 - X_{1\text{H}}$  to high precision. In addition, for small  $\tau_n$  there are very few neutrons which survive weak freeze-out and little helium is produced. The red star in Fig. 5 denotes the values of  $\eta$  and  $\tau_n$  in our Universe and lies on the 25% contour. We can see that in both Figs. 4 and 5, the contours are flat horizontally and regularly spaced vertically in the local area of each red star. The standard formula [14] relating  $n/p$  to helium and hydrogen holds in this local vicinity

$$Y_P = \frac{2n/p}{1 + n/p}, \quad (28)$$

$$X_{1\text{H}} = 1 - Y_P, \quad (29)$$

where  $n/p$  is a function of  $\tau_n$  and independent of  $\eta$ .

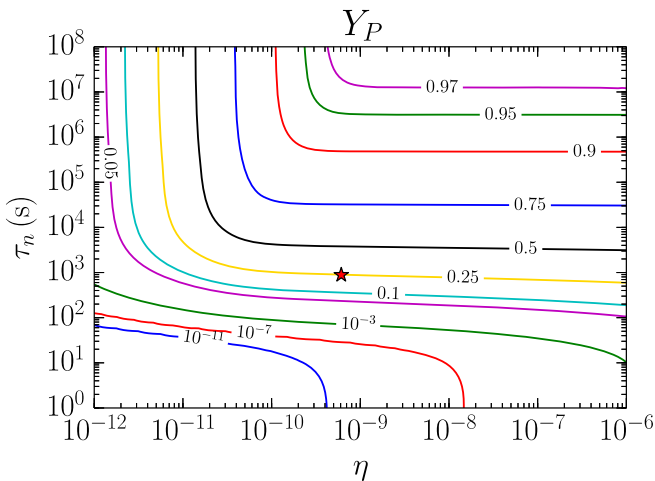


FIG. 5. Contours of constant mass fraction of helium-4 in the  $(\eta, \tau_n)$  plane, where  $\eta$  is the baryon-to-photon ratio, and  $\tau_n$  is the mean neutron lifetime (in seconds). The red star indicates the location of our Universe in the diagram. Little helium is produced during BBN for the lower left part of the diagram (small  $\eta$  and  $\tau_n$ ). In contrast, the mass fraction of helium becomes large (and, hence, problematic) in the upper right part of the figure (large  $\eta$  and  $\tau_n$ ).

In fact, the relationships in Eqs. (28) and (29) hold over the entire parameter space shown in each figure except for the small- $\eta$  and large- $\tau_n$  quadrant. The  $n/p$  ratio is large in this area, but the reaction rates are slow, and so  $Y_P$  is underproduced with respect to the relation in Eq. (28). Figure 6 shows contours of constant deuterium mass fraction in the  $\tau_n$  versus  $\eta$  plane. In the upper left quadrant, we see that  $X_D$  reaches the 10% level, roughly 4 orders of

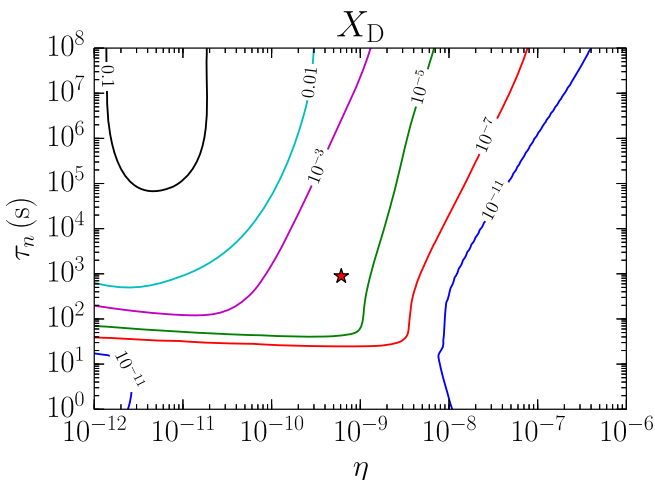


FIG. 6. Contours of constant mass fraction of deuterium in the  $(\eta, \tau_n)$  plane, where  $\eta$  is the baryon-to-photon ratio, and  $\tau_n$  is the mean neutron lifetime (in seconds). The red star indicates the location of our Universe in the diagram. Only trace amounts of deuterium are produced by BBN over the entire plane, except for the upper left part of the figure where  $\tau_n$  is large and  $\eta$  is small.

magnitude larger than the calculation using the values of  $\eta$  and  $\tau_n$  from our Universe.  $n/p$  is still largely preserved, as a deuteron has the same ratio of neutrons to protons as a  ${}^4\text{He}$  nucleus. One issue regarding deuterium, which may be relevant for habitability, is the abundance of water. We do not know the minimum hydrogen abundance for life-sustaining water or if there is such a nonzero minimum. Reference [11] argues that a weakless universe with a low value of  $\eta$  and  $n/p \simeq 1$  does not preclude abundant water due to a relatively large abundance of deuterium. In the weaker universes in the upper left quadrant of Fig. 6,  $X_{\text{H}}$  is larger than  $X_{\text{D}}$ , so there is no problem with a lack of hydrogen in this area of the parameter space. Figure 4 shows that the upper right quadrant of the parameter space suffers from a small  $X_{\text{H}}$ , which is coincident with small  $X_{\text{D}}$  in Fig. 6. Therefore, deuterium is not a solution to the problem of a lack of hydrogen for water in a weaker universe.

We have only included the  $\beta$ -decay rates and  $n \leftrightarrow p$  rates in the weak sector of our nuclear-reaction network, but we can give a qualitative description of what could occur in the presence of other weak interaction rates. In a weakful universe, neutrinos can interact with nuclei through neutral and charged-current processes which could yield rates comparable to the strong and electromagnetic nuclear interactions. (These are not included in the current code.) We included examples of weak interactions with deuterons in Eqs. (3)–(7). Nuclear excited states begin a few MeV above the ground. At temperatures comparable to the nuclear excited states, the strong and electromagnetic nuclear rates are fast enough to keep the lightest nuclei in NSE. We would expect that enhanced weak interactions would keep the nuclear abundances in NSE to lower temperatures. This would not necessarily cause a decrease in the *total*  $n/p$  ratio, as nuclear reactions would supplement the  $n \leftrightarrow p$  rates in keeping  $n/p$  in equilibrium. For example, the neutrino charged-current interaction with deuterons, Eq. (6), gives a secular abundance of

$$Y_{\text{D}} \sim Y_p^2 \frac{n_b}{(mT)^{3/2}} e^{(2m_p - m_{\text{D}})/T} \quad (30)$$

$$\sim Y_p^2 \eta \left(\frac{T}{m}\right)^{3/2} e^{(2m_p - m_{\text{D}})/T}, \quad (31)$$

where  $Y_p$  is the free-proton abundance and  $m$  is the baryon mass. If we assume  $Y_p$  is still of order unity, we see that we can have a significant deuterium abundance at low temperature as  $2m_p > m_{\text{D}}$ . If this is the case, then BBN would result in significant production of deuterium and perhaps heavier nuclei at small  $\tau_n$  rather than resulting in nearly all  ${}^1\text{H}$ . We stress that this is a NSE expression and, therefore, a rough approximate, as under these conditions, the Universe will not be in NSE.

#### IV. WEAKER AND WEAKFUL STARS

We computed evolutionary models of weaker and weakful stars with the stellar evolution code MESA. We created nuclear-reaction networks that reflected a different strength of the weak force by multiplying the  $pp$  and  $pep$  reaction rates by the inverse of the ratio of the neutron lifetime to that in our Universe ( $\tau_{n,0}/\tau_n$ ). Even at the smallest value of  $\tau_n$  we consider, the  $D(p,\gamma)^3\text{He}$  reaction is fast compared with the  $p(p,e^+\nu)D$  reaction (seconds versus days), so we retain MESA’s treatment of the two as a single reaction where every  $pp$  reaction is immediately followed by a  $D$ - $p$  reaction to produce  $^3\text{He}$ . For sufficiently large  $\tau_n$ , we make an additional change to reflect the fact that beta decays in the nuclear-reaction chains will be longer than the lifetime of the star. In this situation, we delete the CNO reactions and the beta decays of  $^7\text{Be}$  and  $^8\text{B}$  from the nuclear-reaction network. The nuclear reactions in later stages of stellar evolution are all strong reactions, so they do not need to be changed.

In the results of our simulations, weaker and weakful stars can be characterized by the dominant energy-producing process powering them. This process varies with the neutron lifetime, stellar mass, and composition but follows some general patterns. In this section, we consider four general cases: first, zero metallicity (population III) and solar metallicity (population I) stars at constant  $\eta$  holding the cosmological parameters constant. Then, we consider zero metallicity and solar metallicity at a constant  $^4\text{He}$  fraction, effectively adjusting  $\eta$  to keep the  $^4\text{He}$  fraction produced by BBN as nearly constant as possible. A constant  $Y_p$  combined with a small  $\tau_n$  requires a value of  $\eta$  larger than the range we explore, and for a sufficiently small  $\tau_n$ , it may be unphysical. Nonetheless, we examine this scenario as a useful point of reference to give a fuller picture of the nuclear processes at work. Stars in small- $\tau_n$  universes would likely form with a near 100%  $^1\text{H}$  composition and would have a lifetime  $\sim 33\%$  longer than the ones we model. We consider a range of  $\tau_n$  ranging from the age of the Universe (at which point, free neutrons survive to the epoch of star formation, and the scenario is functionally equivalent to the weakless universe) down to the limit of  $10^{-8}$  to  $10^{-4}$  s, at which our models of stellar evolution break down. We also note the point at which our models of BBN break down.

Figure 7 shows the main sequence for stars over the range of  $\tau_n$  we study from  $10^{-6}$  to  $10^7$  s. The latter is virtually identical to the main sequence at long  $\tau_n$  out to the point where the CNO cycle shuts down because this is the dominant process in this range (see Sec. IVA). In this figure, we plot only population I stars in the constant- $\eta$  case, because the main sequence does not look significantly different in the other cases, except for being bluer for population III, as expected. In other words, stars look fairly similar over a wide range of  $\eta$  and  $\tau_n$  as long as they

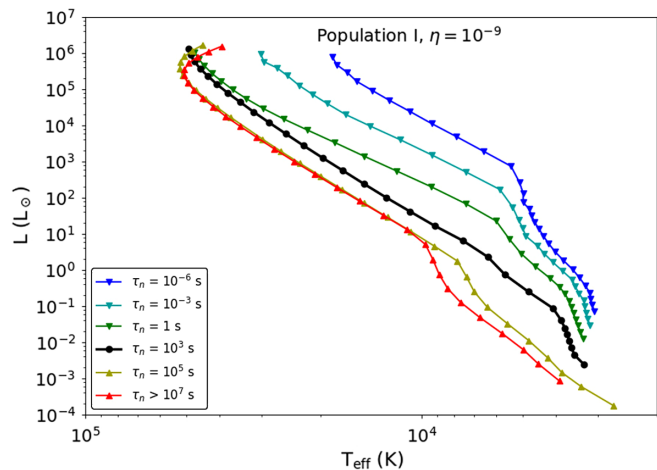


FIG. 7. H-R diagram showing the stellar main sequence for universes with different strengths of the weak interaction. The curves show the main sequence for universes with neutron lifetimes ranging from  $10^{-6}$  s (blue) to  $10^7$  s (red). The stellar masses range from  $100 M_\odot$  down to the minimum mass appropriate for the given universe (as indicated in Fig. 9). Universes with neutron lifetimes longer than  $10^7$  s have essentially identical main sequences, which are that of the weakless limit. Universes with lifetimes shorter than  $10^6$  s involve new nuclear processes relating to neutrino interactions and cannot be modeled with existing stellar evolution codes. All stellar models use the starting composition for population I stars in universes with  $\eta = 10^{-9}$  (see text).

actually attain core hydrogen burning, which is the longest stage of their life cycle and, thus, comprises the main sequence over most of the parameter space we study. A longer neutron lifetime (and a weaker weak force) makes the main sequence bluer but with a similar shape. A shorter neutron lifetime makes the main sequence both redder and steeper, approaching the Hayashi track, where more efficient strong-burning stars fall [11]. A detailed study of the effects of varying the strength of the weak force is given in the following subsections.

##### A. Dominant nuclear processes

This parameter study also requires a clear definition of what a star is. In some parts of the parameter space, “stars” will form with a large fraction of deuterium. This means that deuterium burning will be much more important than in our Universe, and long-lived deuterium-burn objects could exist. This raises the question of how to distinguish a star from a brown dwarf in such a case. For the purpose of this paper, we define a deuterium-burning object to be a star if it has a composition of at least 2% deuterium by mass, for two reasons. First, it is approximately the minimum deuterium fraction required for a minimum-mass star to have a main-sequence lifetime of 1 Gyr, and, thus, it is the lowest deuterium fraction that is important for habitability purposes. Second, as  $\tau_n$  increases to infinity with  $\eta$

remaining the same as in our Universe, the limiting fraction of light hydrogen is also  $\sim 2\%$ , which provides a nice symmetry with our deuterium fraction limit. A deuterium fraction of  $\geq 2\%$  never occurs in either of our constant- $\eta$  cases (see Fig. 6), but it occurs in both of our constant- $Y_p$  cases for  $\tau_n \geq 3000$  s.

Stars can be classified into distinct domains in  $M - \tau_n$  space according to the most important nuclear process that powers them. Perhaps surprisingly, a large part of the parameter space allows long-lived stars to form, although the nuclear processes may vary greatly. We map out these domains in all four of our cases in Figs. 8–11.

A few of the domains are nearly identical in all four cases. If the neutron lifetime is shorter than in our Universe, the  $pp$  chain will be more rapid, and main-sequence stars will run more efficiently, although nuclear-burning rates will not be significantly faster. Stars will reach an equilibrium sooner by switching on earlier in the collapse process, resulting in slightly cooler but brighter stars, analogous to strong-burning stars. The effect on the minimum stellar mass appears to be statistically insignificant and obscured by the limitations of MESA in calculating models for stars so far from those in our Universe. However, one notable effect is that with the  $pp$  chain

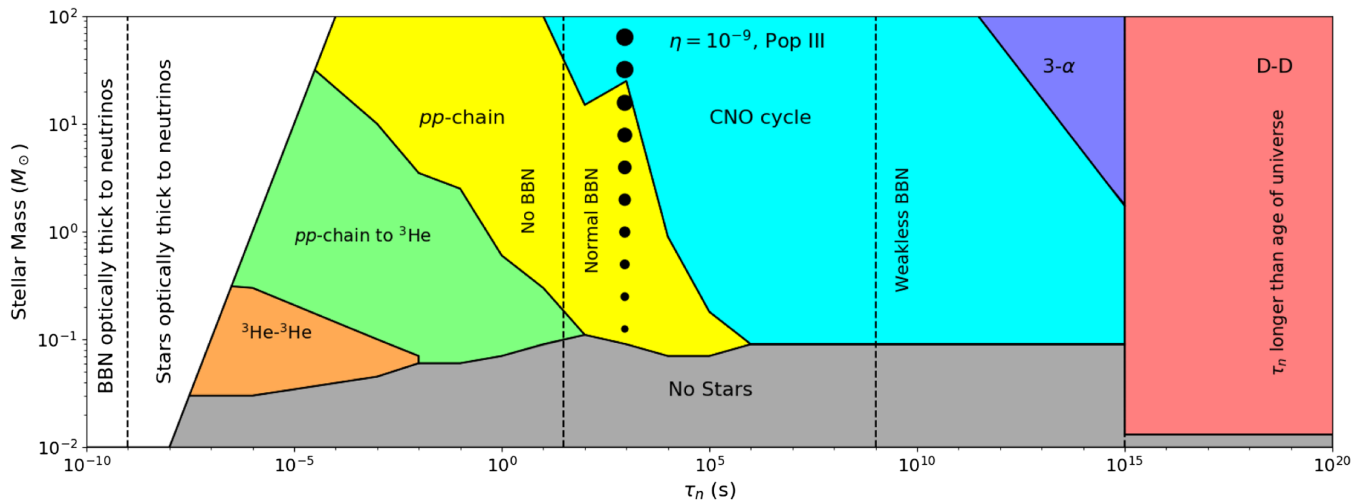


FIG. 8. Regions denoting dominant nuclear processes in population III stars in the space of stellar mass and neutron lifetime. We define the dominant process as the process that powers the star for the longest fraction of its lifetime, so some adjacent regions may undergo the same series of stages of nuclear burning but for different periods of time. For this plot, the baryon-to-photon ratio  $\eta$  of our Universe is maintained, such that regions with high neutron lifetimes are extremely  ${}^4\text{He}$  rich. The gray region denotes parts of the parameter space where long-lived nuclear-powered stars cannot exist. In the white region, the optical depth of stars (and BBN at the far left) to neutrinos is greater than unity, and we cannot simulate nuclear processes with the new neutrino interactions that this introduces.

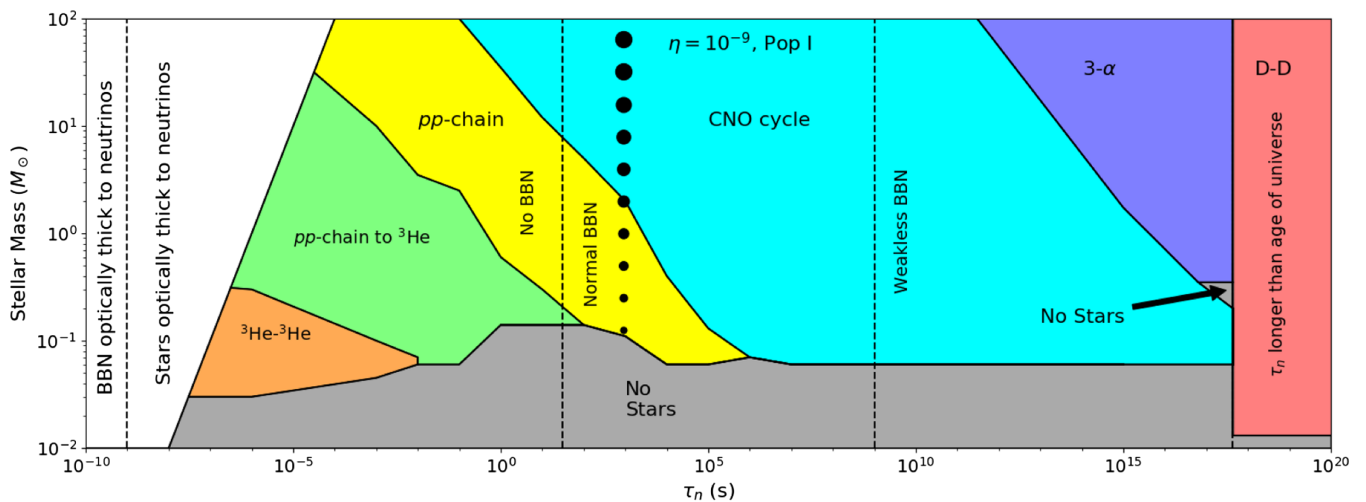


FIG. 9. Same as Fig. 8 but for population I stars, resulting in a more prominent CNO cycle and more neutron decay by the time of star formation.

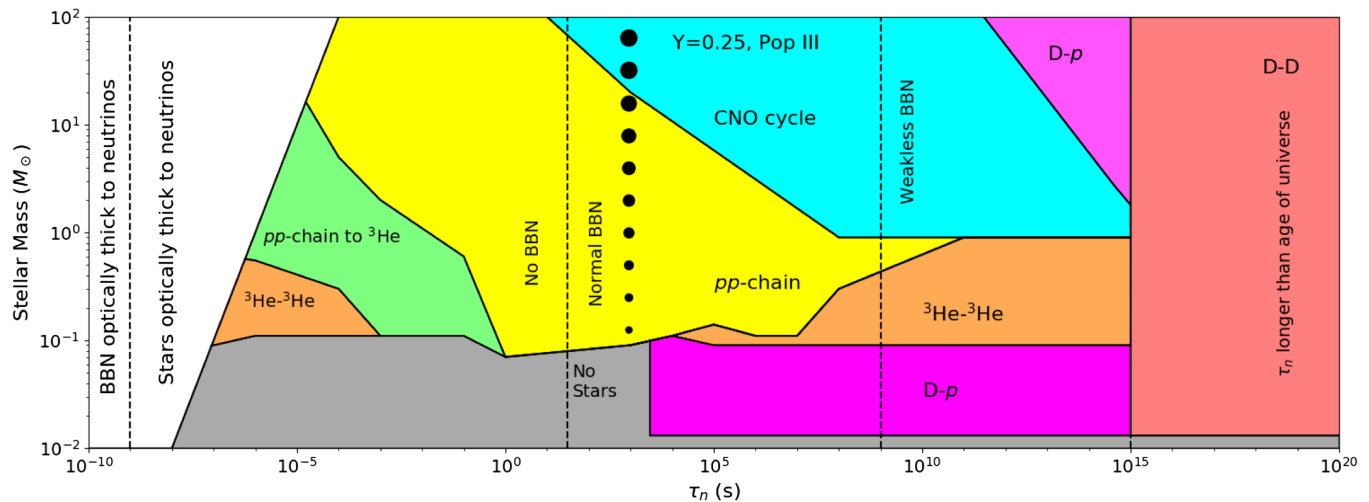


FIG. 10. Same as Fig. 8 but with  $\eta$  allowed to vary so that the helium fraction from BBN,  $Y_p$ , is held constant. In this scenario, if  $\tau_n > 3000$  s, brown dwarfs will form with enough deuterium to become long-lived nuclear-burning objects defined as stars for the purposes of this paper.

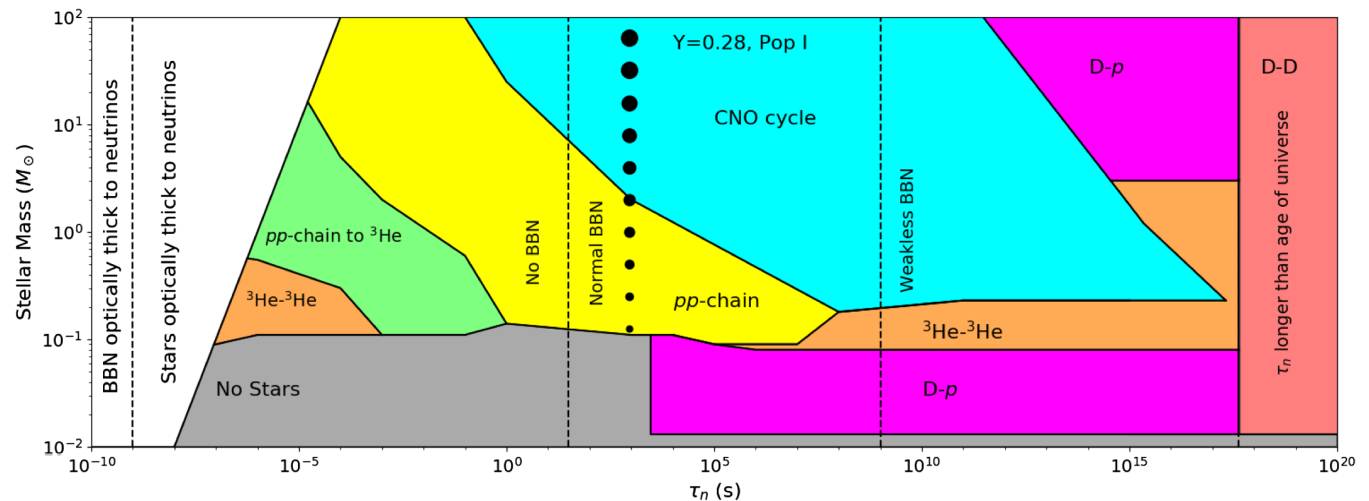


FIG. 11. Same as Fig. 10 but for population I stars, resulting in a more prominent CNO cycle and more neutron decay by the time of star formation.

being more efficient, it dominates over the CNO cycle at much higher masses. For population I stars, the  $pp$  chain dominates up to  $\sim 20 M_\odot$ .

We note that in MESA there can be a considerable margin of error in the boundaries of the domains, most notably in the minimum stellar mass. For example, for stars in our Universe, the smallest mass that MESA correctly simulates with hydrogen fusion is  $0.12 M_\odot$  compared with  $0.08 M_\odot$  for real stars. Thus, the jagged edges seen in a few of the boundaries are probably artifacts of the code and not statistically significant.

Another effect of a stronger weak force is that if  $\tau_n < 30$  s, then BBN will process nearly all baryons into free protons because neutrons will decay before nuclei can

form. However, this will only have the effect of causing the first generation of stars to be made of 100% hydrogen. (For this range, we must set  $Y_p = 0$  in all four cases.)

For even shorter neutron lifetimes, the  $p(p, e^+)D$  step of the  $pp$  chain will be faster than the  ${}^3\text{He}({}^3\text{He}, 2p){}^4\text{He}$  step, and hydrogen burning will occur in two stages: first, the  $pp$  and  $D-p$  reactions to produce  ${}^3\text{He}$ , and second,  ${}^3\text{He}$  burning to produce  ${}^4\text{He}$ . The point at which this occurs varies with mass from  $\tau_n \sim 1$  s for the smallest stars to  $\tau_n \sim 10^{-6}$  s for the largest, as the reaction rates vary differently with the temperature.

Interestingly, the  ${}^3\text{He}$ -burning stage is fairly consistent in timescale regardless of  $\tau_n$ ; for a  $1 M_\odot$  star, it consistently lasts about 500 Myr. Thus, in some parts of the parameter

space (specifically, low mass and a short neutron lifetime), the  ${}^3\text{He}$ -burning stage of a star's life cycle will last longer, while in other parts, the  $pp$ -burning stage will last longer. Because we are addressing the phenomenological aspect of how stars appear in a weakful universe for the largest portion of their lives, we color these two cases as separate regions.

At the opposite end of the scale, if the neutron lifetime is longer than the age of the Universe (for which we have adopted the somewhat short  $10^{15}$  s for population III stars and the present age of the Universe for population I stars), stars will form with a majority of their hydrogen in the form of deuterium and will be powered by D-D fusion. Such universes will approach the appearance of the weakless universe discussed in Ref. [11].

The most important difference between the population III ( $Z = 0$ ) and population I ( $Z = 0.02$ ) cases is that the CNO cycle is more dominant in population I stars. The CNO cycle can still operate in metal-free stars, however. This occurs if the  $pp$  chain is weak enough that the star's core reaches a temperature of 100 MK before  $pp$  burning begins. At this temperature, the  $3\text{-}\alpha$  process rate will be sufficient to produce a trace ( $\sim 10^{-9}$ ) of CNO material. This  $3\text{-}\alpha$  rate is not sufficient to support the star on its own, but at this temperature, the CNO rate is high enough to do so even for trace amounts [39]. The other major difference in the young Universe where population III stars form is that stars can form with large amounts of deuterium with shorter neutron lifetimes (and, thus, fewer neutrons to form deuterium) than population I stars.

There are two major differences between the constant- $\eta$  and constant- $Y_p$  cases. First, in the constant- $\eta$  case, the deuterium fraction produced by BBN never exceeds 2%, so we do not count any low-mass deuterium-burning stars in these cases. The other difference is that over much of the parameter space, constant- $\eta$  stars are denser than in our Universe. This is because stars in universes with a longer neutron lifetime and the same baryon abundance will form with a greater amount of helium. This higher density results in smaller minimum masses for all nuclear processes including, for example, allowing even low-mass stars to undergo CNO burning.

Generally, as the weak force is made weaker, stars will transition from the  $pp$  chain to the CNO cycle as their main power source, with the crossover point (which is  $1.3 M_\odot$  in our Universe) occurring at lower masses. At the same time, the minimum mass for  $pp$  burning increases until it reaches the minimum mass for CNO burning. The minimum CNO-burning mass is lower than in our Universe even for a similar composition (for which it falls at  $0.23 M_\odot$ ) because with a weaker  $pp$  chain, the core is able to contract further and reach a higher temperature before reaching an equilibrium state. In the constant- $\eta$  cases, the minimum CNO-burning mass for the denser stars that occurs there is even lower, at  $0.06 - 0.09 M_\odot$ .

The rate of the CNO cycle normally depends on the strong-burning rates of proton capture reactions. However, it also involves two weak decays that are very fast on stellar timescales:  ${}^{13}\text{N}$  and  ${}^{15}\text{O}$ , both of which have lifetimes of minutes in our Universe. As long as these decays remain fast relative to the lifetime of the star, the CNO cycle is not affected by the strength of the weak force. However, if these decays are longer than the CNO timescale, then the CNO cycle will be suppressed.

At solar metallicities, stars have on the order of 1 CNO nucleus for every  $\sim 100$   ${}^4\text{He}$  nuclei produced. In stars where the CNO cycle dominates, this necessarily means that the CNO timescale is on the order of 1% of the main-sequence lifetime. For the most massive stars, the CNO timescale is, thus, on the order of 10 000 years. The  ${}^{13}\text{N}$  and  ${}^{15}\text{O}$  decay times will be comparable to the CNO timescale for massive stars at  $\tau_n \sim 3 \times 10^{11}$  s and longer for less massive stars. If the weak force is weaker than this, the CNO cycle shuts off, and the  $pp$  chain is very weak, leaving the  $3\text{-}\alpha$  process as the dominant energy source for massive stars in this region of the parameter space.

For population III stars, the CNO abundance will be much smaller at  $\sim 10^{-9}$ , and the CNO timescale will be proportionately shorter: as little as  $3 \times 10^4$  s for the most massive stars. The  $3\text{-}\alpha$  process will dominate at significantly shorter  $\tau_n$  in this case.

The minimum mass for helium burning also depends on the stellar density. For the constant- $\eta$  case, in the helium-rich high- $\tau_n$  region where it is most important, the minimum mass is  $0.35 M_\odot$ , similar to our Universe. For the constant- $Y_p$  case, which is more hydrogen rich, the minimum mass is  $1.2 M_\odot$ . If the neutron lifetime is sufficiently long, stars smaller than this mass will form with the CNO cycle switched off.

These combined factors allow a potential gap in the stellar mass function for certain neutron lifetimes, where no significant nuclear processes are available to them. These are stars for which the neutron lifetime is too long for the CNO cycle to function but too short for significant deuterium to remain to produce deuterium-powered stars, and are too small to fuse helium. This gap appears in the population I region plot for the constant- $\eta$  case (Fig. 9).

However, this applies differently to the constant- $Y_p$  case. Here, for  $\tau_n > 3000$  s, stars form with significant amounts of deuterium approaching 10%, and deuterium fusion becomes an important stellar process. Brown dwarf-mass objects will be low-mass D- $p$  burning stars by our definition. More massive stars larger than  $\sim 0.1 M_\odot$  will undergo a second stage of fusion, burning  ${}^3\text{He}$  to  ${}^4\text{He}$ . This process produces surplus protons, which can only be incorporated into  ${}^4\text{He}$  by being converted to neutrons by weak reactions, so still more massive stars will undergo a third CNO-burning stage, converting the remaining hydrogen to helium. This mass limit varies from  $0.23$  to  $0.9 M_\odot$  depending on metallicity. For these objects, the

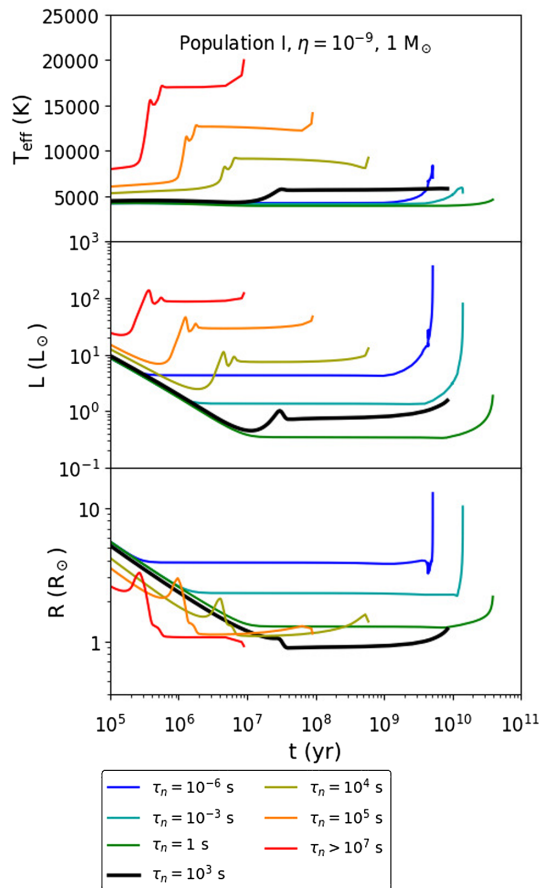


FIG. 12. Evolution of the effective temperature, luminosity, and radius of a  $1 M_{\odot}$  star in universes with constant  $\eta$  and a neutron lifetime ranging from  $10^{-6}$  to  $10^7$  s. Neutron lifetimes longer than  $10^7$  s do not have a significant influence on stellar evolution. Most of the differences in stellar evolution between models are due to the helium fraction of the star.

CNO-burning phase is the longest and produces the most energy. In the upper right region where the  $3\text{-}\alpha$  process dominates for deuterium-poor stars,  ${}^3\text{He}$  burning is again the dominant process for these deuterium-rich stars.

### B. Evolutionary tracks

We examine the evolutionary tracks of stars in universes with a range of neutron lifetimes in Figs. 12 and 13. These figures show the evolution of a  $1 M_{\odot}$  star in the constant- $\eta$  case and the constant- $Y_p$  case, respectively, both at solar metallicity. The zero-metallicity cases do not look dramatically different, except for being somewhat hotter and less luminous, as expected for zero-metallicity stars.

In the constant- $\eta$  case, the most significant change when varying the neutron lifetime is in the stellar lifetime. As described above, a longer neutron lifetime leads to a lower hydrogen fraction, which shortens the stellar lifetime. These low-hydrogen stars are also denser, causing them to be hotter and more compact, which further shortens the

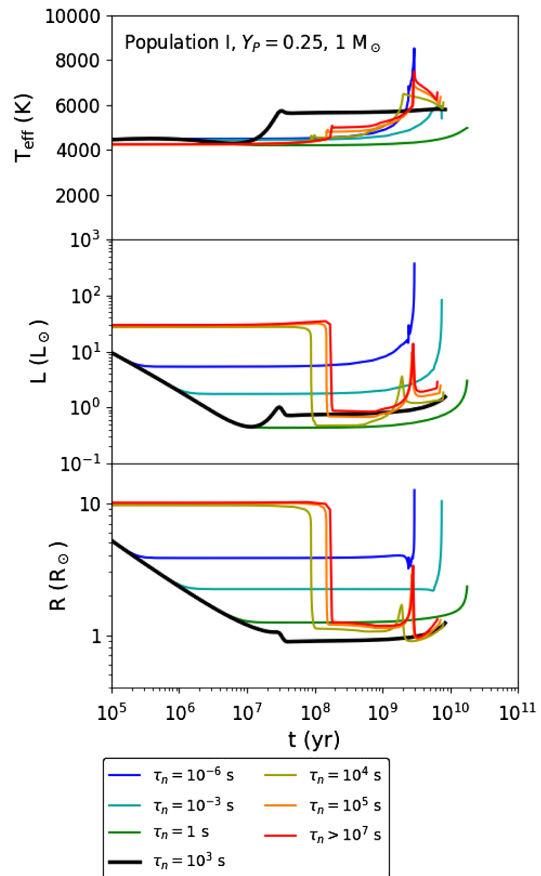


FIG. 13. Same as Fig. 12 but for universes with constant  $Y_p$ . Two distinct types of evolutionary tracks are seen: those for stars with  $\tau_n > 3000$  s, which form with significant amounts of deuterium, and those for stars with  $\tau_n < 3000$  s, which do not.

stellar lifetime. The main sequences approach a limit at  $\tau_n > 10^7$  s, where a  $1 M_{\odot}$  star has a lifetime of  $\sim 10$  Myr, a luminosity of  $\sim 100 L_{\odot}$ , and a surface temperature of  $\sim 17,000$  K. Longer neutron lifetimes result in main sequences nearly identical to  $\tau_n \sim 10^7$  s.

As the neutron lifetime is decreased and hydrogen fusion becomes more efficient along with hydrogen becoming more abundant, stars are longer lived, cooler, and fainter. In particular, the luminosity reaches a minimum at  $\tau_n = 1 - 100$  s, where the initial hydrogen fraction is 100%. Beyond this point, as the ignition temperature of hydrogen becomes still lower, fusion begins and the stars reach equilibrium earlier in the collapse process, resulting in stars that are larger, brighter, and cooler than in our Universe, approaching the properties of red giantlike strong-burning stars like those in a weakless universe.

In the constant- $Y_p$  case, on the other hand, stellar lifetime does not vary greatly with  $\tau_n$ , all falling in the range of 1.5–20 Gyr, because the initial composition is not radically different except for the deuterium abundance. For universes more weakful than our own, we see the same progression of larger, redder stars as the neutron lifetime

decreases. However, for less weakful universes, we see a single, distinctive evolutionary track for all of the models we plot. At constant  $Y_p$ ,  $1 M_\odot$  stars have very similar compositions and the same nuclear processes operating for  $\tau_n$  ranging from  $10^4$  to  $10^{15}$  s. These stars show the three phases of nuclear burning described above.

For these high-deuterium stars, deuterium burning ignites early in the contraction process, resulting in a large, cool, red giantlike star for the first  $\sim 100$  Myr of its life. Once the deuterium is exhausted, the star rapidly contracts to a near-main-sequence state in which  ${}^3\text{He}$  burning occurs, lasting 2–3 Gyr. (This is the most analogous stage to the main sequence in our Universe.) This is followed by a miniature giantlike expansion phase in which the star brightens by a factor of  $\sim 20$  before core hydrogen burning begins (in this case, the CNO cycle), and the star falls back to the main sequence for the longest stage of its life cycle lasting 4–5 Gyr. After this, post-main-sequence evolution occurs similarly to our Universe, since this stage is powered by strong-burning reactions.

To give a clearer picture of the evolution of these deuterium-rich stars, in Fig. 14 we plot the evolutionary track for a representative  $1 M_\odot$  deuterium-rich star on the H-R diagram compared with the evolutionary track for our Sun up to the end of the main sequence. The deuterium-rich star descends the Hayashi track only after the end of deuterium burning to land on the main sequences during

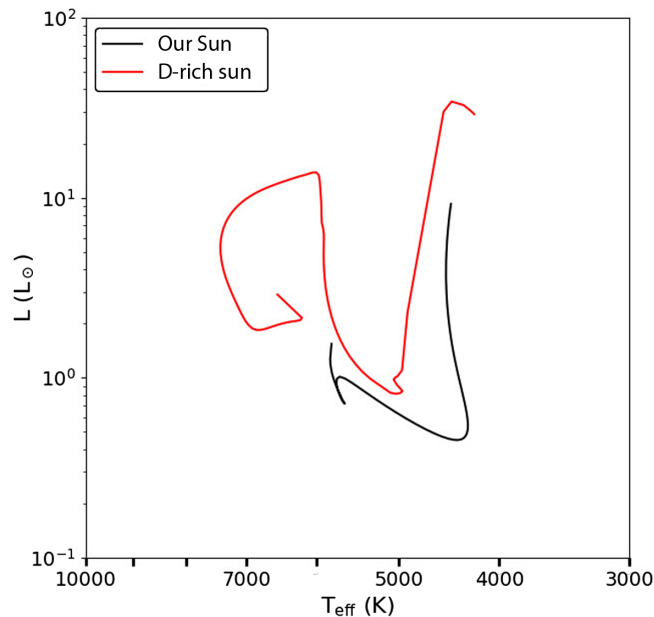


FIG. 14. The two general types of evolutionary tracks for a  $1 M_\odot$  star in universes with constant  $Y_p$  plotted on the H-R diagram. The black curve is the evolutionary track for our Sun, more generally representing stars with  $\tau_n < 3000$  s. The red curve is the evolutionary track for  $\tau_n = 10^8$  s and more generally represents stars with  $\tau_n > 3000$  s.

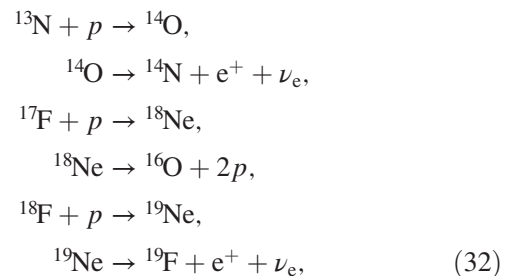
${}^3\text{He}$  burning. The star then expands along a small giantlike branch before contracting again to land higher on the main sequence during core hydrogen burning.

## V. CHEMICAL EVOLUTION AND HABITABILITY

For most of the parameter space considered in this study, chemical evolution proceeds similarly to that in our Universe. The same nuclear reactions provide power in stellar cores, especially during post-main-sequence evolution, although they proceed at different rates. As a result, only the abundances of the lightest isotopes are significantly affected by the strength of the weak force. A stronger weak force results in a lower helium fraction due to much lower helium production during BBN. Such universes could also have a dramatically higher cosmic  ${}^3\text{He}$  abundance because in a large region of the parameter space,  ${}^3\text{He}$  production occurs separately from  ${}^4\text{He}$  production. Meanwhile, a weaker weak force, on the other hand, can result in a lower light hydrogen (proton) abundance and a higher deuterium abundance from BBN.

A stronger weak force would result in core-collapse supernovae being more efficient and dispersing more oxygen and other  $\alpha$  elements because the neutrinos that power them would interact more strongly. However, this trend may reverse for an even stronger weak force as neutrinos would become trapped in the core and, thus, unable to impart sufficient momentum to the overlying gas layers to eject them, which would then cause the supernova to fail [6]. If core-collapse supernovae do function, a stronger weak force would also cause  $r$ -process yields from neutron star mergers to decrease as ( $\beta$ ) decay becomes faster, and the  $r$  process comes to more closely resemble the  $s$  process. Since the  $r$ -process timescale is  $\sim 100$  ms [40] and typical  $\beta$ -decay times on the neutron-rich side of the line of stability are on the order of 10 to  $10^4$  s, the  $r$  process will closely resemble the  $s$  process at  $\tau_n \lesssim 10^{-2}$  s.

For a sufficiently weaker weak force, one important change occurs to chemical evolution in the CNO cycle. If the lifetimes of  ${}^{13}\text{N}$  and  ${}^{15}\text{O}$  are similar to the CNO timescale, it will both slow the CNO cycle as described above and also open up new reaction pathways in the various branches of the cycle:



and so on. With more possibilities to continue adding more protons, it is unclear where the CNO cycle will halt under

typical stellar conditions by ejecting an alpha particle as in the  $^{15}\text{N} + \text{p} \rightarrow ^{12}\text{C} + ^4\text{He}$  step of the CNO-I branch. It may halt at fluorine, as in the hot CNO cycle in our Universe, or it may continue further under cooler conditions. It is plausible that this would result in significantly higher fluorine and neon abundances and less carbon than in our Universe.

Another effect of a weaker weak force is that weaker neutrino interactions are likely to cause core-collapse supernovae to fail, as in the weakless universe. In the weakless universe, elements heavier than oxygen are dispersed essentially only by type Ia supernovae. The core-collapse supernovae needed to produce the  $\alpha$  elements and the neutron stars needed to enact the  $r$  process will not occur in a significantly weaker universe. However, with the weak force still included, the  $s$  process would remain in operation, allowing an additional pathway for heavy elements, although its yields may be lower. The  $s$  process will also come to resemble the  $r$  process if the neutron capture timescale is shorter than typical  $\beta$ -decay times. The  $s$ -process timescale is 5–100 yr [41], so this will occur for  $\tau_n \gtrsim 10^{12}$  s.

Another important consideration to habitability in a universe with a different weak force is stellar lifetime. In the majority of the parameter space, long-lived stars can exist with similar chemical evolution to our Universe, and this presents no significant barrier to habitability. However, in a large minority of the parameter space with large  $\eta$  and large  $\tau_n$ , stars are not long-lived enough for life as we know it to develop due to their low-hydrogen fractions. As in the weakless universe, a low value of  $\eta$  is needed to allow a large hydrogen abundance to survive BBN. However, in this case, with the weak force still operating, stars in these universes are more hostile to life with a long, early deuterium-burning stage with high luminosity, along with the period that would be the main-sequence lifetime of stars in our Universe interrupted by an expansion phase between  $^3\text{He}$  burning and core hydrogen burning. With such a variability in stellar brightness, it is not clear whether a planet orbiting such a star could acquire and retain a large volatile reservoir long enough for life as we know it to develop. It is possible, then, that life in such a universe would be relegated to low-mass stars with deuterium-burning times longer than 1 Gyr that can provide a relatively stable environment, as in the weakless universe.

## VI. CONCLUSION

This paper has considered a class of universes for which the strength of the weak force is vastly different from that in our own region of space-time. We have performed numerical simulations for both big bang nucleosynthesis and stellar evolution using a wide range of possible strengths for the weak force. The overall finding of this study is that universes are remarkably robust to changes in the strength of the weak force, in that a wide range of universes remain

viable. Here we have provided a summary of our specific results (Sec. VI A) along with a discussion of their implications (Sec. VI B).

### A. Summary of results

For the sake of definiteness, we parametrize the strength of the weak force in terms of the neutron lifetime (where  $\tau_n \simeq 885$  s for our Universe). The limit where  $\tau_n \rightarrow \infty$  corresponds to the weakless universe, as would a neutron lifetime longer than the age of the Universe,  $\tau_n > 10^{18}$  s. At the opposite end of the scale,  $\tau_n \leq 10^{-9}$  s leads to substantial changes to nuclear structure. Overall, we consider a range of  $\tau_n$  spanning more than 25 orders of magnitude.

We have studied the epoch of big bang nucleosynthesis in detail using the code BURST. In the limit of large  $\tau_n$ , neutrons do not decay during the epoch of BBN, and the Universe tends to produce a large amount of helium. In order to allow some protons to survive, which is necessary for the Universe to have nuclear fuel and produce water, the baryon-to-photon ratio must be smaller than that of our Universe. For small  $\eta$  and large  $\tau_n$ , BBN allows for substantial amounts of protons, deuterium, and helium. In the limit of small  $\tau_n \lesssim 10$  s, neutrons decay so quickly that the Universe emerges from the BBN epoch with an almost pure hydrogen composition.

We have studied stellar structure and evolution using the state-of-the-art code MESA. Here, the parameter space for stars is broken into four regimes characterized by two variables. The first variable is metallicity, for which we consider both  $Z = 0$  (population III) and  $Z = 0.02$  (population I) metallicities. The second variable determines the starting stellar composition. Here we consider the abundances produced by BBN for constant  $\eta$ , as well as composition characterized by constant helium mass fraction.

Over the allowed range of strengths of the weak force, equivalently varying values of  $\tau_n$ , energy generation in stellar interiors is dominated by a variety of different nuclear reactions (see Figs. 2–5). In the limit of large  $\tau_n$ , universes tend to produce large abundances of deuterium, and stellar energy generation is dominated by deuterium burning. As the weak force becomes stronger, so that  $\tau_n$  is shorter, the  $pp$  chain becomes more effective than the CNO cycle and comes to dominate even at high stellar masses. For sufficiently small values of  $\tau_n$ , the  $pp$  reaction is fast enough (relative to subsequent reactions in the standard  $pp$  chain) that stars experience a new nuclear-burning phase that produces helium-3 as its end product (which is only later burned into helium-4). The boundaries between the different regimes of nuclear burning depend on stellar mass, as expected.

The allowed range of stellar masses is largely insensitive to the strength of the weak force. The upper mass limit taken here to be  $M_{\text{max}} = 100 M_{\odot}$  is set by radiation

pressure and other considerations and does not depend on  $\tau_n$ . The lower mass limit (near  $0.1 M_\odot$ ) is nearly constant for the case of fixed  $\eta$ . For constant helium abundance, universes with larger  $\tau_n$  produce substantial deuterium abundances, which allow small stars to operate through deuterium fusion (D- $p$  burning). As a result, a window opens up for small stars with masses  $0.01 - 0.1 M_\odot$  in universes with  $\tau_n \gtrsim 3000$  sec. These deuterium-rich stars become larger, brighter, and redder at all masses and, thus, resemble red giants in our Universe. For universes with constant  $\eta$ , a large fraction of the hydrogen fuel is already processed into helium during the epoch of BBN so that stars are hotter, brighter, and shorter lived.

In the opposite limit with small  $\tau_n$ , stars operate by burning protons into helium-3 at moderately lower temperatures. Their radii and luminosities are comparable to, but somewhat larger than, those of stars in our Universe, whereas their surface temperatures are relatively unchanged. Consistent with this insensitivity of stellar properties, the main sequences at constant  $\eta$  in the H-R diagram are much like those observed in our Universe. Stellar lifetimes in such universes will be modestly shorter than in our Universe by as much as a factor of a few, although this will be partially mitigated by the higher  $^1\text{H}$  content.

## B. Discussion

The results of this paper show that universes can remain potentially habitable over a wide range of strengths for the weak force. Given the resilient nature of universes subject to these variations, it is useful to consider the range of properties that could render the universe sterile.

In Fig. 3, we have noted that our Universe exists in the middle of a plateau where  $N_{\text{eff}} \simeq 3$ . The neutron lifetime must change by roughly 2 orders of magnitude in either direction for  $N_{\text{eff}}$  to deviate from 3.0. The plateau is a result from the fact that neutrino decoupling occurs before  $e^\pm$  annihilation and after  $\mu^\pm$  annihilation. As we always assume the charged lepton seas are in thermal and chemical equilibrium with the plasma, the mass of the respective particles defines the relevant energy scale for the two epochs. This location of our Universe on the plateau is partly apparent from the relation that  $(G_F^2 m_{\text{pl}})^{-1/3} \sim 1$  MeV, an energy scale between the two lepton mass scales (this is similar to the decoupling energy scale which we took to be 3.0 MeV in Sec. III A). For our Universe, interesting consequences could arise if there exist additional interactions that affect the temperature scale where neutrinos begin to decouple. Neutrino magnetic moments [42] or hidden interactions [43] could lower the decoupling temperature. Figure 3 shows that such an interaction would have to overwhelm the weak interaction by 2 orders of magnitude to produce changes in  $N_{\text{eff}}$ ,

although secret interactions solely within the neutrino seas could have other ramifications on the cosmic microwave background and large-scale structure [44,45]. A changing  $N_{\text{eff}}$  would change the epoch of matter-radiation equality, which would have ramifications for the onset of galaxy formation [46] and large-scale structure [47]. However, neither the low nor high bounds of  $N_{\text{eff}}$  in Eqs. (24) and (25) will dramatically shift the matter-radiation equality before habitability becomes an issue. In light of these facts, we conclude that there does not exist a fine-tuning argument for how  $G_F$  affects the expansion history of the Universe. What is more sensitive to the weak interaction is the primordial abundances, specifically, the ratio of hydrogen to helium. An increase in  $\tau_n$  of 2 orders of magnitude will flip the Universe from hydrogen dominated to helium dominated. We would presume that life requires a nonzero primordial hydrogen component, although we do not know what the strict lower bound may be. Nevertheless, if  $\tau_n$  is large enough, a dearth of hydrogen could be problematic for life.

One way to inhibit life is for the Universe to emerge from BBN with few unbound protons. In the limit of  $\tau_n \rightarrow \infty$ , this occurs at and even somewhat below the value  $\eta_0$  in our Universe. Specifically, for  $\eta = \eta_0 = 6 \times 10^{-10}$ , only  $\sim 1\%$  of the mass of the Universe remains in protons [11]. However, universes with  $\eta < \eta_0$  remain viable even for  $\tau_n \rightarrow \infty$ . We find that it is relatively difficult for BBN processes to compromise the Universe, consistent with previous results [47].

The opposite limit of stronger weak forces is more problematic. Stars cease to operate normally if the neutrinos produced by nuclear reactions become optically thick. This limit depends on stellar mass but requires  $\tau_n \gtrsim 10^{-6}$  s for solar-type stars. Even smaller values of  $\tau_n$  corresponding to an even stronger weak force lead to substantial contributions to the energy budget of nuclei. The strength of the weak interaction required to compromise nuclear structure remains unknown, but the periodic table is likely to be quite different for the regime where  $\tau_n \ll 10^{-10}$  s. In this regime, neutrinos are also optically thick during BBN, so the output of BBN is equally uncertain.

As outlined above, universes continue to be viable when the strength of the weak force is varied over many orders of magnitude. In addition to its ramifications for fine-tuning, these results also provide us with a deeper understanding of how BBN and stellar evolution operate in our Universe. One general trend emerging from this study is that stars are more robust than nuclei. If the laws of physics—in this context, the strength of the weak force—allow for complex nuclei to exist, then stellar interiors are likely to produce them. The reason for this flexibility is that stars can operate using a wide range of different nuclear processes, from the  $pp$  reaction through the weak interaction to deuterium

burning through the strong interaction (and many additional chains in between). Moreover, stars span a wide range of mass (a factor of  $\sim 1000$ ) and can produce an even wider range of densities and temperatures in their cores. This enormous range of available parameter space coupled with the exponential temperature sensitivity of nuclear-reaction rates allows for stars to operate over a wide range of realizations of the laws of physics (see, also, [39,48]).

### ACKNOWLEDGMENTS

We would like to thank Daniele Alves, Vincenzo Cirigliano, George Fuller, and Lillian Huang for useful

discussions. This work was supported by the John Templeton Foundation through Grant No. ID55112: Astrophysical Structures in other Universes and by the University of Michigan. This work was supported in part by the Los Alamos National Laboratory Institutional Computing Program, under the U.S. Department of Energy National Nuclear Security Administration Award No. DE-AC52-06NA25396. Computational resources and services were also provided by Advanced Research Computing at the University of Michigan. E. G. acknowledges support from the National Science Foundation, Grant No. PHY-1630782 and the Heising-Simons Foundation, Grant No. 2017-228.

- 
- [1] P. C. W. Davies, *Mod. Phys. Lett. A* **19**, 727 (2004).  
 [2] J. F. Donoghue, *Annu. Rev. Nucl. Part. Sci.* **66**, 1 (2016).  
 [3] G. F. R. Ellis, U. Kirchner, and W. R. Stoeger, *Mon. Not. R. Astron. Soc.* **347**, 921 (2004).  
 [4] A. Linde, *Rep. Prog. Phys.* **80**, 022001 (2017).  
 [5] M. Rees, *Before the Beginning: Our Universe and Others* (Addison-Wesley, Reading, 1997).  
 [6] B. J. Carr and M. J. Rees, *Nature (London)* **278**, 605 (1979).  
 [7] B. Carter, *Phil. Trans. R. Soc. A* **310**, 347 (1983).  
 [8] J. D. Barrow and F. J. Tipler, *The Anthropic Cosmological Principle* (Oxford University Press, Oxford, 1986).  
 [9] C. J. Hogan, *Rev. Mod. Phys.* **72**, 1149 (2000).  
 [10] M. Rees, *Just Six Numbers: The Deep Forces that Shape the Universe* (Basic Books, New York, 2000).  
 [11] E. Grohs, A. R. Howe, and F. C. Adams, *Phys. Rev. D* **97**, 043003 (2018).  
 [12] R. Harnik, G. D. Kribs, and G. Perez, *Phys. Rev. D* **74**, 035006 (2006).  
 [13] G. Kane, *Modern Elementary Particle Physics* (Cambridge University Press, Cambridge, 2017).  
 [14] E. W. Kolb and M. S. Turner, *The Early Universe* (Addison-Wesley Publishing Co., Reading, MA, 1990).  
 [15] E. Grohs, G. M. Fuller, C. T. Kishimoto, and M. W. Paris, *J. Cosmol. Astropart. Phys.* **5** (2015) 017.  
 [16] B. Paxton, L. Bildsten, A. Dotter, F. Herwig, P. Lesaffre, and F. Timmes, *Astrophys. J. Suppl. Ser.* **192**, 3 (2011).  
 [17] J. N. Bahcall, in *Solar Modeling*, edited by A. B. Balantekin and J. N. Bahcall (World Scientific, River Edge, 1995), p. 1.  
 [18] V. Agrawal, S. M. Barr, J. F. Donoghue, and D. Seckel, *Phys. Rev. D* **57**, 5480 (1998).  
 [19] P. F. Bedaque, T. Luu, and L. Platter, *Phys. Rev. C* **83**, 045803 (2011).  
 [20] L. J. Hall, D. Pinner, and J. T. Ruderman, *J. High Energy Phys.* **12** (2014) 134.  
 [21] M. S. Smith, L. H. Kawano, and R. A. Malaney, *Astrophys. J. Suppl. Ser.* **85**, 219 (1993).  
 [22] R. V. Wagoner, W. A. Fowler, and F. Hoyle, *Astrophys. J.* **148**, 3 (1967).  
 [23] L. Kawano, NASA STI/Recon Technical Report No. 25163, 1992, p. 92.  
 [24] S. Hannestad, *New J. Phys.* **6**, 108 (2004).  
 [25] C. A. Bertulani and T. Kajino, *Prog. Part. Nucl. Phys.* **89**, 56 (2016).  
 [26] S. Mukohyama, *Phys. Lett. B* **473**, 241 (2000).  
 [27] E. Grohs and G. M. Fuller, *Nucl. Phys.* **923B**, 222 (2017).  
 [28] E. Grohs and G. M. Fuller, *Nucl. Phys.* **911B**, 955 (2016).  
 [29] D. N. Blaschke and V. Cirigliano, *Phys. Rev. D* **94**, 033009 (2016).  
 [30] D. A. Dicus, E. W. Kolb, A. M. Gleeson, E. C. G. Sudarshan, V. L. Teplitz, and M. S. Turner, *Phys. Rev. D* **26**, 2694 (1982).  
 [31] G. M. Fuller, W. A. Fowler, and M. J. Newman, *Astrophys. J. Suppl. Ser.* **42**, 447 (1980).  
 [32] J. E. Carlstrom *et al.* (CMB-S4 Collaboration), American Astronomical Society Meeting, No. 228, 2016.  
 [33] M. Fukugita and T. Yanagida, *Phys. Lett. B* **174**, 45 (1986).  
 [34] E. K. Akhmedov, V. A. Rubakov, and A. Y. Smirnov, *Phys. Rev. Lett.* **81**, 1359 (1998).  
 [35] S. Davidson, E. Nardi, and Y. Nir, *Phys. Rep.* **466**, 105 (2008).  
 [36] M. Drewes, B. Garbrecht, P. Hernández, M. Kekic, J. Lopez-Pavon, J. Racker, N. Rius, J. Salvado, and D. Teresi, *Int. J. Mod. Phys. A* **33**, 1842002 (2018).  
 [37] M. Sher, *Phys. Rep.* **179**, 273 (1989).  
 [38] P. A. R. Ade *et al.* (Planck Collaboration), *Astron. Astrophys.* **594**, A13 (2016).  
 [39] F. C. Adams and E. Grohs, *Astropart. Phys.* **91**, 90 (2017).  
 [40] R. A. Surman, M. R. Mumpower, G. C. McLaughlin, R. Sinclair, W. R. Hix, and K. L. Jones, in *Capture Gamma-Ray Spectroscopy and Related Topics*, edited by P. E. Garrett *et al.* (World Scientific, Singapore, 2013), pp. 304–313.  
 [41] J.-I. Matsuda, R. S. Lewis, and E. Anders, *Astrophys. J.* **237**, L21 (1980).  
 [42] N. Vassh, E. Grohs, A. B. Balantekin, and G. M. Fuller, *Phys. Rev. D* **92**, 125020 (2015).

- [43] J. Barranco, O.G. Miranda, and T.I. Rashba, *J. High Energy Phys.* **12** (2005) 021.
- [44] D. Baumann, D. Green, J. Meyers, and B. Wallisch, *J. Cosmol. Astropart. Phys.* **1** (2016) 007.
- [45] F. Forastieri, M. Lattanzi, G. Mangano, A. Mirizzi, P. Natoli, and N. Saviano, *J. Cosmol. Astropart. Phys.* **07** (2017) 038.
- [46] L. A. Barnes, P.J. Elahi, J. Salcido, R. G. Bower, G.F. Lewis, T. Theuns, M. Schaller, R. A. Crain, and J. Schaye, *Mon. Not. R. Astron. Soc.* **477**, 3727 (2018).
- [47] F.C. Adams, S. Alexander, E. Grohs, and L. Mersini-Houghton, *J. Cosmol. Astropart. Phys.* **3** (2017) 021.
- [48] F. C. Adams, *J. Cosmol. Astropart. Phys.* **2** (2016) 042.